Accepted Manuscript

Combining structure- and property-based optimization to identify selective FLT3-ITD inhibitors with good antitumor efficacy in AML cell inoculated mouse xenograft model

Hao Heng, Zhijie Wang, Hongmei Li, Yatian Huang, Qingyuan Lan, Xiaoxing Guo, Liang Zhang, Yanle Zhi, Jiongheng Cai, Tianren Qin, Li Xiang, Shuxian Wang, Yadong Chen, Tao Lu, Shuai Lu

PII: S0223-5234(19)30430-1

DOI: https://doi.org/10.1016/j.ejmech.2019.05.021

Reference: EJMECH 11331

To appear in: *European Journal of Medicinal Chemistry*

Received Date: 21 March 2019

Revised Date: 3 May 2019

Accepted Date: 6 May 2019

Please cite this article as: H. Heng, Z. Wang, H. Li, Y. Huang, Q. Lan, X. Guo, L. Zhang, Y. Zhi, J. Cai, T. Qin, L. Xiang, S. Wang, Y. Chen, T. Lu, S. Lu, Combining structure- and property-based optimization to identify selective FLT3-ITD inhibitors with good antitumor efficacy in AML cell inoculated mouse xenograft model, *European Journal of Medicinal Chemistry* (2019), doi: https://doi.org/10.1016/j.ejmech.2019.05.021.

This is a PDF file of an unedited manuscript that has been accepted for publication. As a service to our customers we are providing this early version of the manuscript. The manuscript will undergo copyediting, typesetting, and review of the resulting proof before it is published in its final form. Please note that during the production process errors may be discovered which could affect the content, and all legal disclaimers that apply to the journal pertain.

ACCEPTED MANUSCRIPT

ACCEPTED MANUSCRIPT

Combining structure- and property-based optimization to identify selective FLT3-ITD inhibitors with good antitumor efficacy in AML cell inoculated mouse xenograft model

Hao Heng[†, #], Zhijie Wang[†, #], Hongmei Li[†, #], Yatian Huang[†], Qingyuan Lan[†], Xiaoxing Guo[†], Liang Zhang[†], Yanle Zhi[I], Jiongheng Cai[‡], Tianren Qin[‡], Li Xiang[‡], Shuxian Wang[‡], Yadong Chen[§, *], Tao Lu[¶], Shuai Lu[†, *]

[†] School of Science, China Pharmaceutical University, Nanjing 211198, P.R. China.

[I] School of Pharmacy, Henan University of Chinese Medicine, Zhengzhou 450046, P. R. China

[‡] School of Pharmacy, China Pharmaceutical University, Nanjing 210009, P.R. China.

[§] Laboratory of Molecular Design and Drug Discovery, China Pharmaceutical University, Nanjing, 211198, P.R. China.

[¶] State Key Laboratory of Natural Medicines, China Pharmaceutical University, Nanjing 210009, P.R. China

Abstract

FLT3 mutation is among the most common genetic mutations in acute myeloid leukemia (AML), which is also related with poor overall survival and refractory in AML patients. Recently, FLT3 inhibitors have been approved for AML therapy. Herein, a series of new compounds with pyrazole amine scaffold was discovered, which showed potent inhibitory activity against FLT3-ITD and significant selectivity against both FLT3-ITD and AML cells expressing FLT3-ITD. Compound **46**, possessing the most promising cellular activity, blocked the autophosphorylation of FLT3 pathway in MV4-11 cell line. Furthermore, the apoptosis and downregulation of P-STAT5 were also observed in tumor cells extracted from the MV4-11 cell xenografts model upon compound **46** treatment. Compound **46** was also metabolically stable *in vitro* and suppressed tumor growth significantly in MV4-11 xenografts model *in vivo*. Compound **46** showed no toxicity to the viscera of mice and caused no decrease in body weight of mice. In conclusion, the results of this study could provide valuable insights into discovery of new FLT3 inhibitors, and compound **46** was worthy of further development as potential drug candidate to treat AML.

Key words: FLT3-ITD; inhibitor; selectivity; AML

Introduction

Acute myeloid leukemia (AML) is one severe type of tumor that occurs mostly in children and adolescents [1], causing about ten thousand deaths in the United States in 2017, with a 5-year survival rate of 27%.[2] It is reported that approximately 30% of AML patients harbored the Fms-like tyrosine kinase 3 (FLT3) mutation.[3] Normally, FLT3 is one member of type III receptor tyrosine kinase that is mainly expressed in hematopoietic and lymphocytes cells, and regulates the growth, differentiation and apoptosis of cells. [4] Pathologically, FLT3 mutations are often capable of the autophosphorylation and excessive activation of its downstream signaling pathways, including signal transducer and activator of transcription 5 (STAT5), Ras/mitogen-activated protein kinase (MAPK) and phosphatidylinositol 3 kinase (PI3K) / AKT pathway.[5] FLT3 mutations can be divided into two types, *i.e.* internal-tandem duplication (ITD) in the juxtamembrane domain of kinase [6] and tyrosine kinase domain (TKD)[7] point mutations. After standard chemotherapy, AML patients with FLT3-ITD mutation had a worse prognosis than those with wild-type FLT3.[8-10] Actually, both types of mutations not only correlate with negative prognosis, but also contribute greatly to the drug resistance for current FLT3 inhibitors.[9, 11] Therefore, FLT3, especially mutant FLT3, has attracted numerous interests to develop targeting inhibitors toward AML therapy.

According to their binding modes, FLT3 inhibitors can be categorized into type I and type II.[12] Crenolanib, sorafenib, quizartinib, gilteritinib and midostaurin (**Figure 1**) are the representative and advanced inhibitors. The combination of midostaurin with standard chemotherapy can effectively prolong the overall survival of AML patients with FLT3 mutations.[13] Quizartinib has an excellent effect on FLT3-ITD mutation, and can effectively prevent fatal bone marrow suppression, prolonging the survival and improving the life quality of AML patients.[14] Sorafenib was reevaluated in several clinical trials for AML, and improved the outcomes for patients with FLT3-ITD.[15-17] Despite of the reported FLT3 inhibitors,[18] novel chemical entities that are effective and selective against either FLT3-ITD and FLT3-TKD alone or concurrent mutations[19] are still urgently needed due to the fast developing drug resistance. [20]

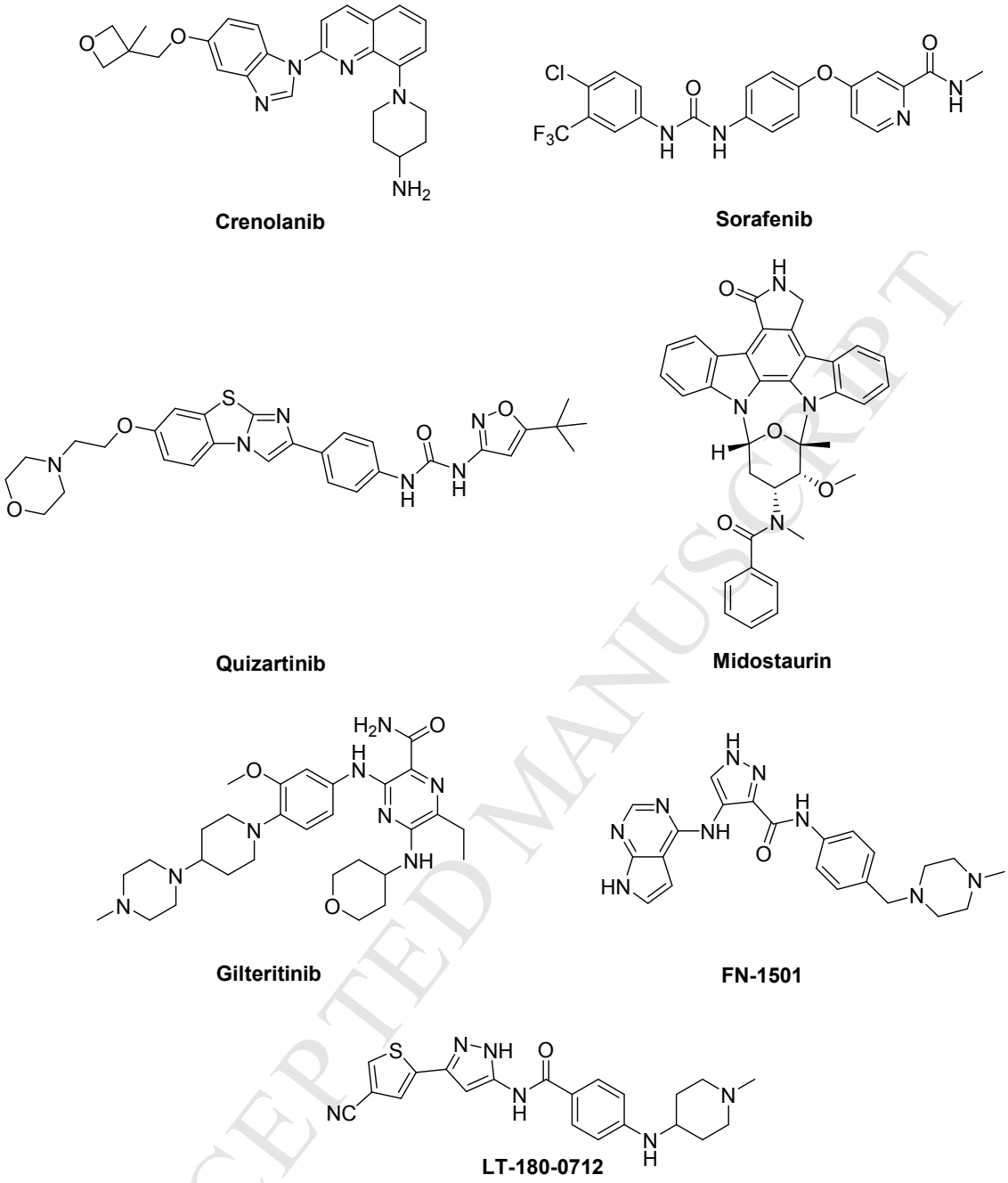

Figure 1. Represented FLT3 inhibitors and hit compound **LT-180-0712** of this work.

In our previous efforts on FLT3 inhibitor research, several potent compounds have been identified, among which **FN-1501** is being under evaluation in phase I clinical trial.[21, 22] However, **FN-1501** was also potent CDKs inhibitors, making it not a selective FLT3 inhibitor. To discover more selective FLT3-ITD inhibitors, a virtual screening was performed based on our in-house molecule database, and a hit compound (**LT-180-0712**) with good selectivity against FLT3 was identified by us.[23] Herein, a series of new pyrazole amines with improved cellular activity was discovered by hit to lead optimization, of which a representative compound showed

high FLT3 selectivity from enzyme and cell-based assays as well as significant anti-AML efficacy *in vivo*.

Chemistry

Scheme 1. Synthesis of compounds **8-18**.

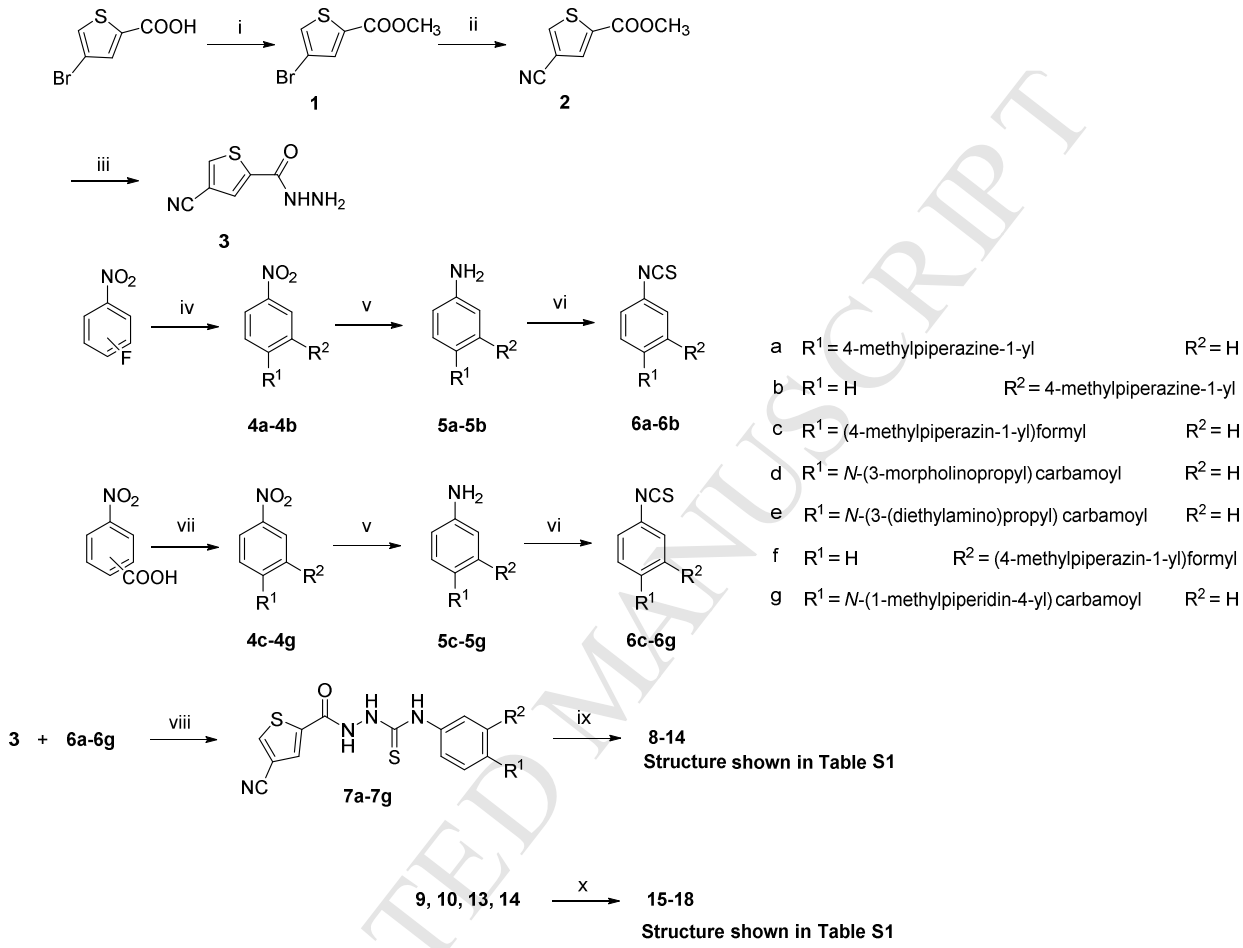

Reagents and conditions: (i) $SOCl_2$, MeOH, reflux; (ii) CuCN, KI, DMF, reflux; (iii) $NH_2NH_2 \cdot H_2O$, EtOH, 45 °C; (iv) Amines, Et_3N, DMF, r.t.; (v) Fe, NH_4Cl, EtOH, reflux; (vi) $CSCl_2$, DCM, $NaHCO_3$, H_2O, 0 °C; (vii) Amines, HATU, DIPEA, DMF; (viii) Pyridine, EtOH, reflux; (ix) $Hg(OAc)_2$, EtOH, reflux; (x) NaOH, 30% H_2O_2, EtOH, 50 °C.

Compounds **8-18** were prepared by a general approach shown in **Scheme 1**. 4-Bromo-thiophene-2-carboxylic acid was used as the starting material to synthesize compound **3** through a sequence of esterification, cyano substitution and hydrazinolysis.[24] 4-Fluoronitrobenzene or 3-fluoronitrobenzene was used as the starting material to synthesize compounds **4a-4b** through a nucleophilic substitution reaction with the appropriate amines. Reduction of compound **4a-4b** gave compounds **5a-5b**, followed by the reaction with thiophosgene to obtain intermediates **6a-6b**. Amides **4c-4g** were synthesized by coupling 4-nitrobenzoic acid or 3-nitrobenzoic

acid with the related amines. Similar steps were conducted to convert **4c-4g** to **6c-6g** as used in the synthesis of **6a-6b**. Reaction of compound **3** with intermediates **6a-6g** followed by cyclization gave title compounds **8-14**. The hydrolysis of corresponding compounds gave title compounds **15-18**.[25, 26] Compounds **23-27** and **45-54** were prepared by a general approach shown in **Scheme 2**. The pyrazolamines (**20** and **21a-21f**) were synthesized using similar procedures to those in **Scheme 1**. Coupling reaction catalyzed by palladium gave intermediates **22a-22i**. Then, title compounds **23-26** and **45-54** were obtained by the amination reactions of intermediates **20**, **21a-21f** and **22a-22i**. Hydrolysis of hit compound **LT-180-0712** gave compound **27**. Accordingly, compounds **28-34** and **38-44** (**Scheme 3**) were synthesized using similar procedures to those shown in **Scheme 1** and **Scheme 2**.

Scheme 2. Synthesis of compounds 23-27 and 45-54.

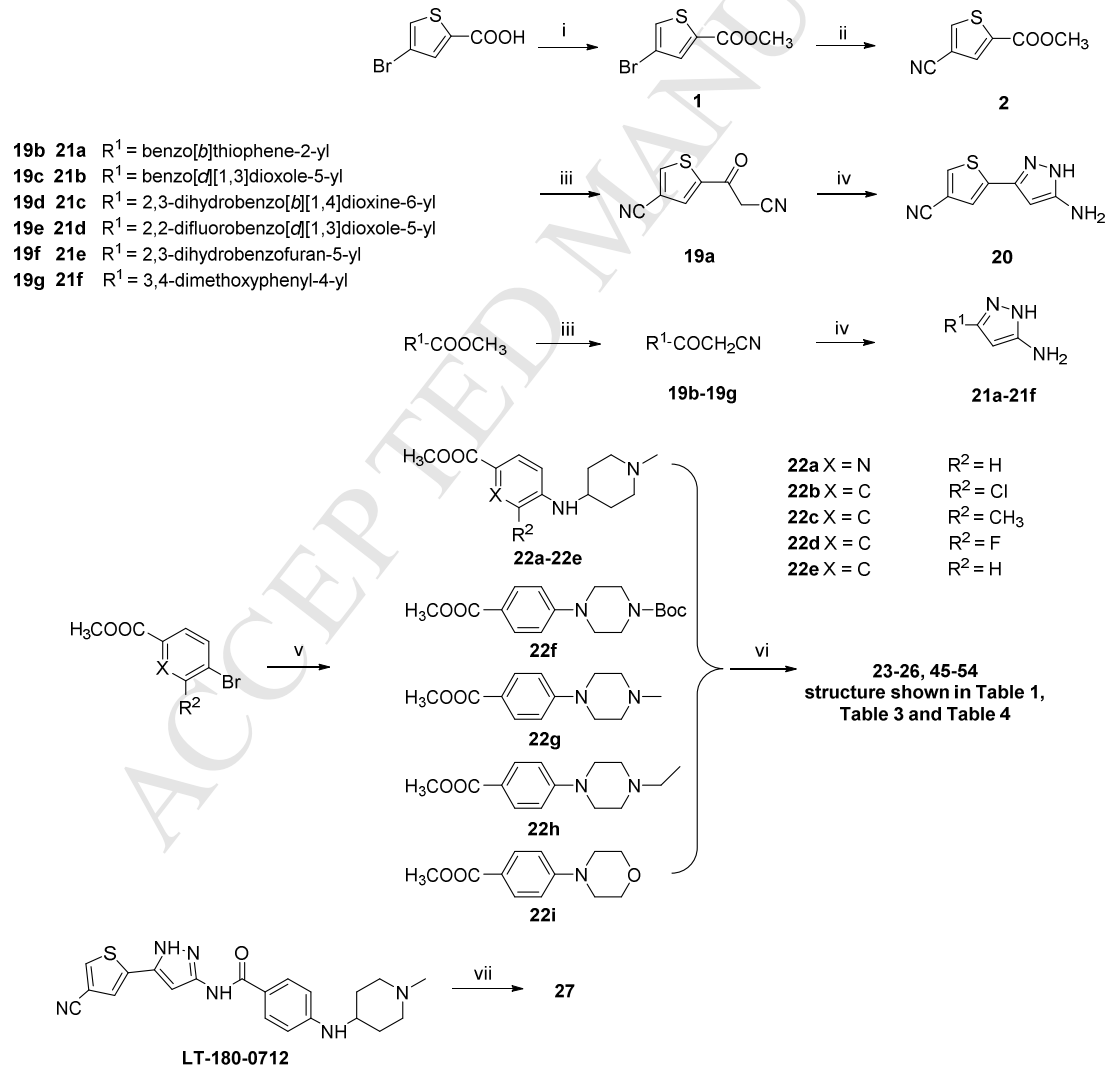

Reagents and conditions: (i) $SOCl_2$, MeOH, reflux; (ii) CuCN, KI, DMF, reflux; (iii) NaH, THF, CH_3CN, reflux; (iv) $NH_2NH_2 \cdot H_2O$, EtOH, reflux; (v) Amines, $Pd(OAc)_2$, BINAP, Cs_2CO_3, Tol,

90 °C; (vi) **20** or **21a-21f**, $Al(CH_3)_3$, Tol, 90 °C; (vii) KOH, EtOH, reflux.

Scheme 3. Synthesis of compounds 28-34 and 38-44.

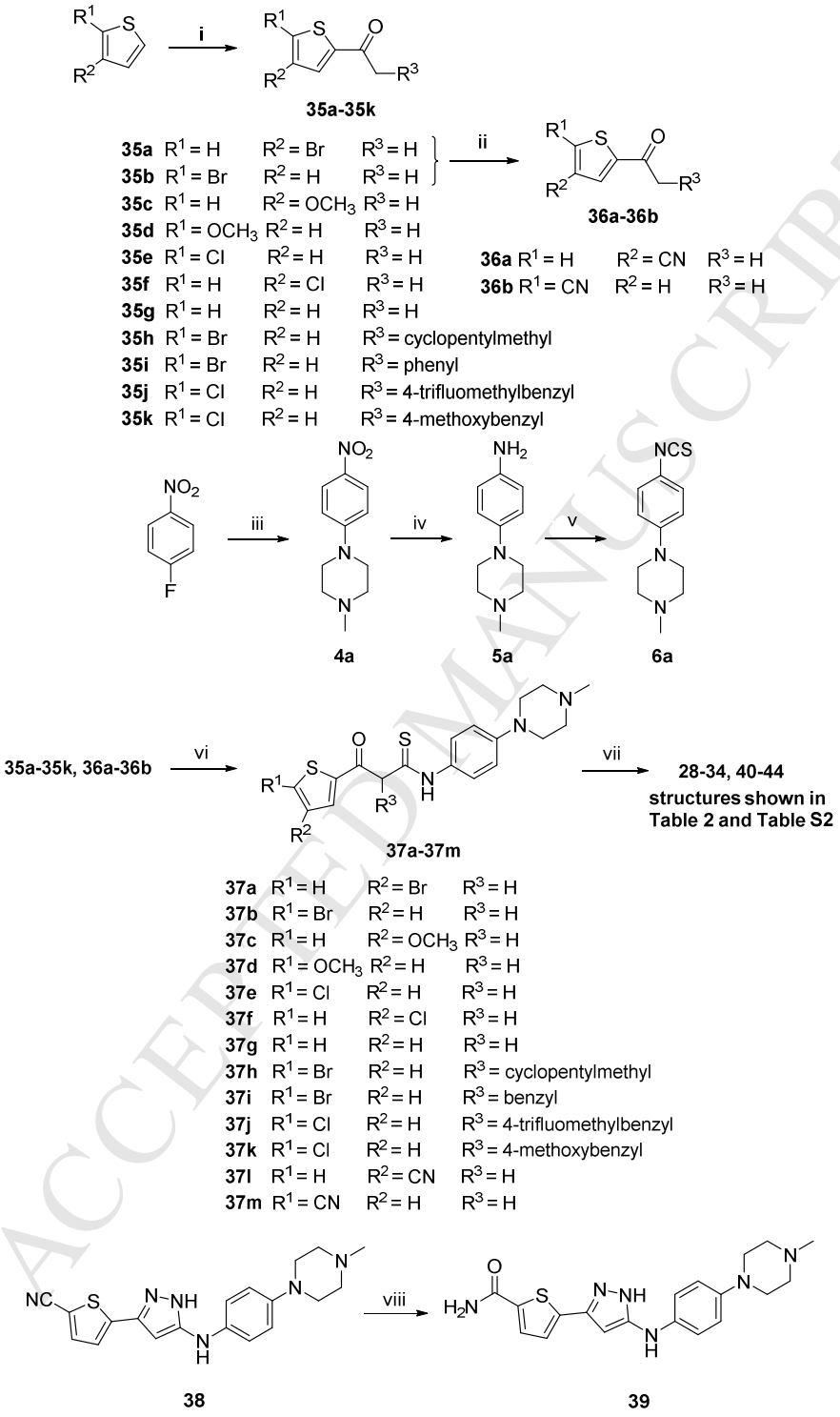

Reagents and conditions: (i) Intermediates **35a-35g**: acetic anhydride, $HClO_4$, 0 °C; Intermediates **35h-35k**: corresponding carboxylic acids, H_3PO_4, TFAA, CH_3CN, r.t.; (ii) CuCN, KI, DMF, reflux; (iii) 1-Methylpiperazine, Et_3N, DMF, r.t.; (iv) Fe, NH_4Cl, EtOH, reflux; (v) $CSCl_2$, DCM, $NaHCO_3$, H_2O, 0 °C; (vi) Intermediate **6a**, NaH, THF/DMF, 0 °C; (vii)

$NH_2NH_2 \cdot H_2O$, EtOH, reflux; (viii) KOH, EtOH, reflux.

Results and discussion

Structure and activity relationship (SAR). Previously, we found a potent and selective FLT3-ITD inhibitor **LT-180-0712** (IC_{50} = 0.9400 nM), but its cellular activity against MV4-11 cell line was moderate (IC_{50} = 917 nM).[23] To discover new selective FLT3-ITD inhibitors with improved cell efficacy, we firstly tried to increase the cellular activity by structure-based optimization on **LT-180-0712** and maintain the kinase inhibitory activity. However, the initial oxadiazole bioisosteres of **LT-180-0712** showed nearly eliminated FLT3-ITD inhibitory activity (**Table S1**), suggesting that the pyrazole ring was indispensable for the enzymatic efficacy. To verify this speculation, we docked compound **8** and **LT-180-0712** to FLT3 in active form (since no activated FLT3 crystal structure was revealed, the homology model [23] that we constructed before was used). As shown in **Figure 2**, neither key hydrogen bonding interaction nor π-cation interaction formed between compound **8** and FLT3.

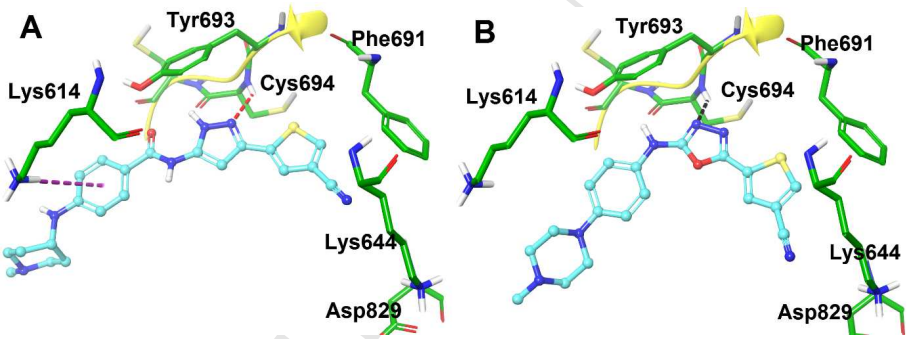

Figure 2. Docking binding mode of **LT-180-0712** (A) and compound **8** (B) in FLT3 homology model. Yellow ribbon represents hinge region. Red dash line represents hydrogen bond; magenta dash line π-cation interaction; black dash line represents the close contact of atoms. Carbon atoms of the FLT3 residues and the ligand are shown in green and cyan color, respectively.

Hence, we focused on the study of pyrazole compounds. As shown in **Table 1**, when keeping the cyano group unchanged, the introduction of chlorine, fluorine atom or methyl group at position 3 of benzene ring (**23-25**) made FLT3-ITD inhibitory potency decrease in different degrees. The sharp attenuation of kinase activity for compounds **23** and **24** was probably due to unfavorable steric clash between the chlorine atom or methyl group and Tyr693 of FLT3 and thus lack of key hydrogen boning with hinge region (**Figure 3A** and **3B**). Both replacing the benzene ring with pyridine ring (**26**) and introducing hydrogen bonding donor on thiophene ring (**27**) only slightly attenuated the FLT3-ITD inhibitory activity (IC_{50} = 8.963 and 3.120 nM, respectively). However, cell potencies of compounds **26** and **27** against MV4-11 cells were moderately improved (IC_{50} = 298 and 244 nM, respectively). This discrepancy

on kinase and cell activities reminded us that weak cellular potency of this kind of compounds was probably due to the unfavorable transmembrane capacity. Hence, solubility and transmembrane properties of those compounds were predicted. The data (**Table 1**) showed that compounds **23-27** and **LT-180-0712** possessed weaker predicted Caco-2 cell permeability and lower logP values than the clinical FLT3 inhibitors did, such as Crenolanib, Midostaurin, Sorafenib and Quzartinib. Therefore, we turned to use the property-based optimization strategy.

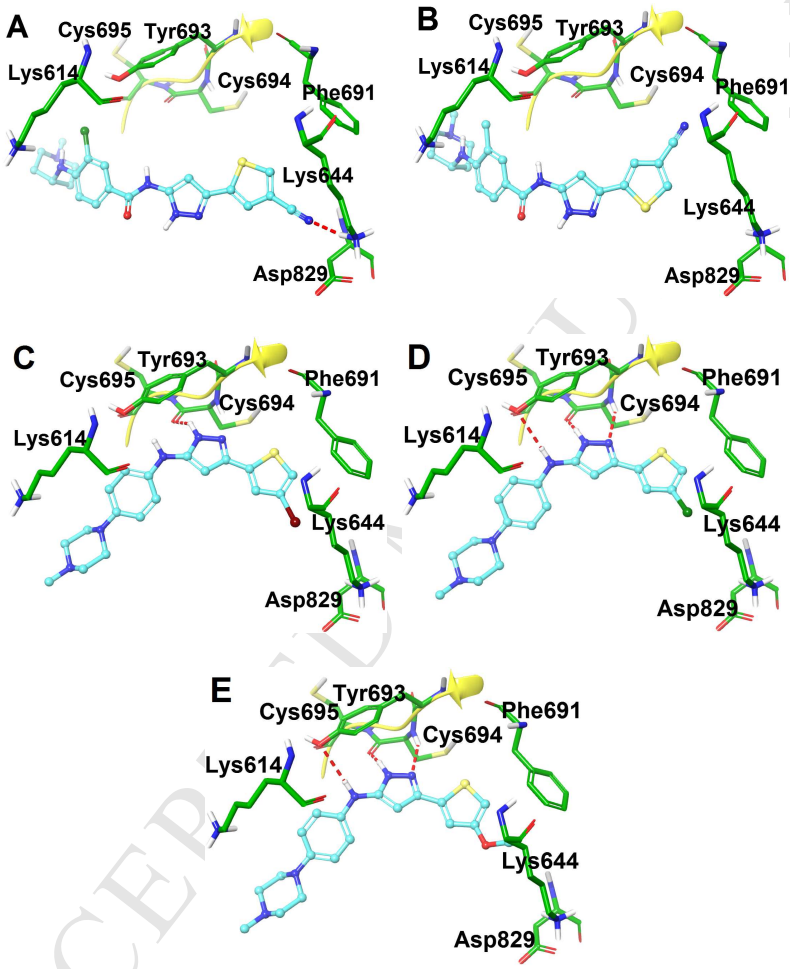

Figure 3. Docking binding mode of compounds **23** (A), **24** (B), **29** (C), **30** (D) and **31** (E) in FLT3 homology model. Yellow ribbon represents hinge region. Red dash line represents hydrogen bond; black dash line represents the close contact of atoms. Carbon atoms of the FLT3 residues and the ligand are shown in green and cyan color, respectively.

Table 1. Structures and biological data of compounds **23-27.**

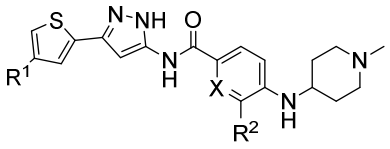

Cpd.	R^1	R^2	X	FLT3-ITD IC_{50} (nM) [a]	MV4-11 IC_{50} (nM) [b]	PlogP [d]	PCaco [e]
23	CN	Cl	C	1198±102	- [c]	2.929	43.612
24	CN	CH_3	C	398.7±10.4	-	2.869	53.13
25	CN	F	C	39.61±2.3	-	2.709	42.4
26	CN	H	N	8.963±1.1	298±11	2.44	29.013
27		H	C	3.120±0.8	244±16	2.171	18.308
LT-180-0712				0.9400±0.02	917±27	2.532	44.735
Crenolanib						4.041	359.609
Midostaurin						5.394	2266.241
Sorafenib				1.300±0.3	1.59±0.15	4.11	322.725
Quzartinib						4.553	110.126

[a] In the presence of 10 μM ATP, the values are the mean from three independent experiments (± SD); [b] the values are the mean from three independent experiments (± SD); [c] not determined; [d] predicted logP; [e] predicted Caco-2 cell permeability in nm/second.

Considering that the amide linker between pyrazole and benzene ring may contribute negatively to transmembrane capacity, a -NH- group was used as the new linker (**Table 2**). Although enzymatic activities of compound **28** decreased by more than 10 times, compounds **29**, **30** and **31** possessed comparable FLT3-ITD inhibitory potency with hit compound, and their binding modes in FLT3 (**Figure 3C-3E**) were also similar with that of hit compound. Therefore, the -NH- linker was acceptable to maintain kinase activity. More importantly, compounds **29** and **30** also displayed six times higher cell efficacy (IC_{50} = 130 nM and 148 nM, respectively) than hit compound did. Indeed, compounds **29** and **30** had obviously increased predicted logP values and Caco-2 cell permeability (**Table 2**), which probably facilitated these two compounds to transfer into MV4-11 cells and inhibited cell growth. Consistently, compound **31** that had lower predicted logP values and Caco-2 cell permeability than compounds **29** and **30**, showed decreased cellular potency (IC_{50} = 756 nM).

Next, we continued to investigate various substituents with different volume or electrostatic property on thiophene ring. When changing substitutions on position 5 of thiophene ring (**32**, **33**, **34, 38, 39**), only compound **32** with 5-Br group showed 10-fold decreased kinase activity and the other compounds displayed maintained kinase activities, perhaps due to too close distance between the bromine atom of compound **32** and Phe691 of FLT3 (**Figure 4A**). Compounds **33** and **34** showed better cellular activities (IC_{50} = 85 and 80 nM, respectively) than compounds **38** and **39**, which was consistent with their differences in the predicted logP and Caco-2 cell

permeability values. Unexpectedly, compound **40**, with no substitution at thiophene ring, also demonstrated potent enzyme inhibitory activity (IC_{50} = 0.327 nM), suggesting that simple substituents on thiophene were not necessary to intermolecular binding (**Figure 4B**). And higher predicted logP and Caco-2 cell permeability values and the improved cell efficacy (IC_{50} = 74 nM) were concurrent for compound **40**.

However, substitution on pyrazole ring (**41**-**44**) led to eliminated potency against FLT3-ITD and MV4-11 cells (**Table S2**), though these compounds had high predicted Caco-2 cell permeability. Molecular docking results indicated that the cyclopentylmethyl group (**41**) formed unfavorable steric clashes with Leu616 and Val624 of FLT3, which probably caused the intermolecular binding unstable (**Figure S1**), suggesting unsubstitution on the pyrazole ring was optimal.

Table 2. Structures and biological data of compounds **28**-**34** and **38**-**40.**

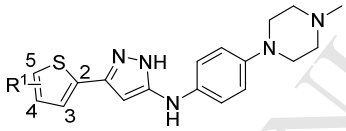

Cpd.	R^1	FLT3-ITD IC_{50} (nM) [a]	MV4-11 IC_{50} (nM) [b]	PlogP	PCaco
28	4-CN	30.12±1.6	-[c]		
29	4-Br	1.711±0.42	130±11	4.361	643.97
30	4-Cl	0.7991±0.09	148±12	4.283	642.941
31	4-OCH_3	1.960±0.1	756±31	3.782	488.549
32	5-Br	48.31±1.3	-		
33	5-Cl	1.503±0.17	85±6	4.275	637.811
34	5-OCH_3	1.711±0.2	80±4	4.026	454.706
38	5-CN	2.006±0.59	261±18	2.918	92.801
39		3.212±0.88	418±24	1.988	37.645
40	H	0.3270±0.05	74±3	3.78	639.025
Sorafenib		1.300±0.3	1.59±0.15	4.11	322.725

[a] In the presence of 10 μM ATP, the values are the mean from three independent experiments (± SD); [b] The values are the mean from three independent experiments (± SD); [c] Not determined.

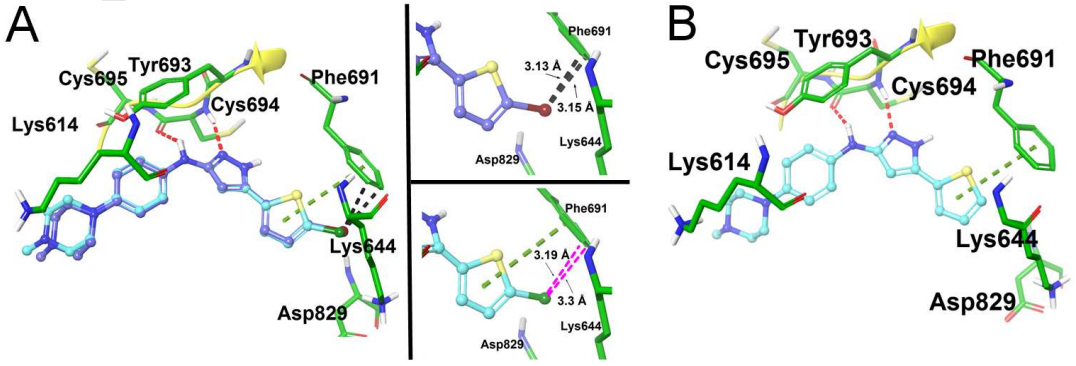

Figure 4. Overlapped docking binding mode of compounds **32** and **33** (A) and binding mode of

compound **40** (B) in FLT3 homology model. Yellow ribbon represents hinge region. Red dash line represents hydrogen bond; green dash line represents π-π interaction; black dash line represents the close contact of atoms. Carbon atoms of the FLT3 residues and the ligand are shown in green and cyan color, respectively.

Since the simple modification on hit compound only enhanced the cellular potency by 12 folds (**40**), we wondered whether other moieties could replace thiophene ring and further improve the cellular potency. Hence, the scaffold hopping was adopted on the thiophene ring (**Table 3**) because substitutions on this ring were generally tolerated in kinase activity. Initially, fusing a benzene ring with thiophene led to the obvious decrease in enzymatic and cellular activity (**45**). Further, the thiophene was replaced with benzodioxol and 2,3-dihydrobenzodioxin ring (**46** and **47**), respectively. Compound **46** showed ~3 times more potent cellular efficacy (IC_{50} = 27 nM) than compound **40** did. However, compound **47** with the expanded fused-ring system, possessed 10 times weaker cell efficacy than compound **46** did. Subsequently, we investigated the analogues of compound **46**. The addition of two fluorine atoms at the benzodioxol moiety (**48**) caused a sharp decline in cell potency and enzyme activity. And substituting an oxygen atom with CH_2 group (**49**) in benzodioxol ring also had a negative consequence on cell potency (IC_{50} = 339 nM). When the oxygen containing ring was open (**50**), both enzyme and cell inhibitory potencies decreased dramatically. The data implied that structural modification on the benzodioxol moiety was detrimental. Therefore, the benzodioxol ring was reserved as the optimal substituent.

Table 3. Structures and biological data of compounds **45-50.**

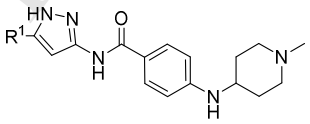

Compound	R^1	FLT3-ITD IC_{50} (nM) [a]	MV4-11 IC_{50} (nM) [b]	PlogP	PCaco
45	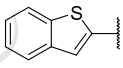	10.51±1.2	335±23	4.731	221.618
46	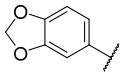	1.336±0.3	27±2	3.439	219.834
47	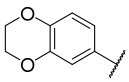	12.50±2.1	236±9	3.276	225.442
48	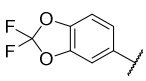	123.9±10.3	1175±106	3.808	224.695
49	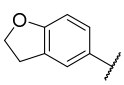	25.88±1.6	339±3	4.024	227.32

50	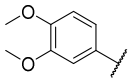	63.65±1.9	335±12	3.573	224.836
Sorafenib		1.300±0.3	1.59±0.15	4.11	322.725

[a] In the presence of 10 μM ATP, the values are the mean from three independent experiments (± SD); [b] The values are the mean from three independent experiments (± SD).

In order to investigate the effect of hydrophilic amines on the activity, compounds **51**-**54** with varying cyclic amines were synthesized. The data (**Table 4**) showed that piperazine and substituted piperazine (**51**-**53**) were tolerable to kinase activity but made cell efficacy decrease moderately. For morpholine (**54**), it made an obvious reduction in the kinase and cell activities. Hence, we kept *N*-methyl piperidine as the current optimal group in hydrophilic region of FLT3. The SAR was collectively illustrated in **Figure 5**.

Table 4. Structures and biological data of compounds **51-54.**

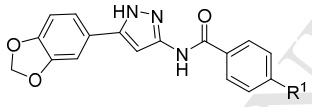

Compound	R^1	FLT3-ITD IC_{50} (nM) [a]	MV4-11 IC_{50} (nM) [b]
51	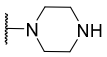	1.518±0.12	62±1
52	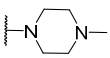	4.434±0.6	54±4
53	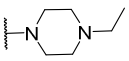	2.773±0.1	64±7
54		8.422±0.25	96±4
Sorafenib		1.300±0.3	1.59±0.15

[a] In the presence of 10 μM ATP, the values are the mean from three independent experiments (± SD); [b] The values are the mean from three independent experiments (± SD).

ACCEPTED MANUSCRIPT

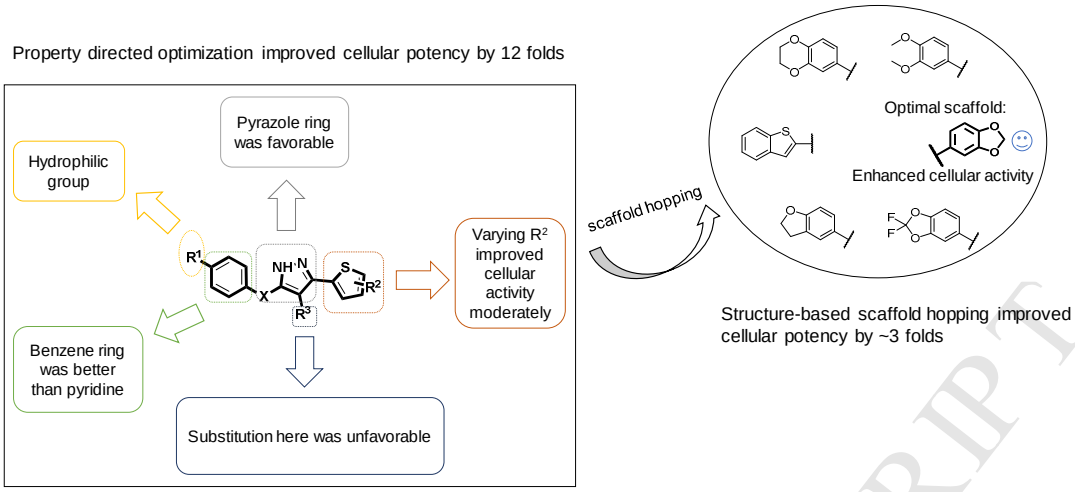

Figure 5. Summarized SAR.

Inhibitory activity of compound 46 against other kinases. We tested FLT3-ITD selectivity of compound **46** over a panel of 48 kinases at the concentration of 0.1 μM. As shown in **Table S3**, only six kinases had an inhibitory rate greater than 60%, which includes FMS and c-kit that are very closely homologous to FLT3. Furthermore, at least 100-fold selectivity of FLT3-ITD over those 6 kinases was observed (**Table 5**). In addition, the high selectivity of compound **46** over c-kit (461-fold) was thought to be beneficial for avoiding the potential synthetic lethal myelosuppreion.[27-30] Moreover, compound **46** almost showed no inhibitory activity against CDKs that were among the targets of **FN-1501**.

As reported,[31, 32] some FLT3 inhibitors were subjected to drug resistance due to FLT3 mutation. Therefore, we tested inhibitory activities of compound **46** against a variety of commonly occurred FLT3 mutants. As shown in **Table 6**, compound **46** suppressed those FLT3-ITD or FLT3-TKD mutants with IC_{50} values lower than 25 nM. Notably, compound **46** inhibited FLT3-D835Y (IC_{50} = 18.71 nM) or FLT3-D835V (*K*d = 7.3 nM) potently, which could cause drug resistance to type II FLT3 inhibitors. [28] And it bound two concurrent FLT3-ITD-TKD mutants with *K*d values around 100 nM. To further validate potency of compound **46** against FLT3 mutants, its antiproliferative activities were investigated in BaF3 cells transformed with FLT3 mutants. The data showed that compound **46** indeed inhibited growth of BaF3 cells harboring FLT3 mutations; while it did not obviously affect the growth of parental BaF3 cells (**Table 7**).

Table 5. IC_{50} of compound **46** against 6 kinases.

Kinase	IC_{50} (nM) [a]
ABL1	1340±102
BTK	161±8

c-Kit	616±13
FMS	247±11
LCK	860±25
TRKA	432±19

[a] Mean value of results from triplicate runs (± SD).

Table 6. Inhibitory efficacy of compound **46** against wild-type FLT3 and several FLT3 mutants.

Kinase	Activity
FLT3	66.75±1.32 [a]
FLT3 (D835Y)	18.71±1.62 [a]
FLT3 (F594_R595insR)	11.22±1.31 [a]
FLT3 (F594_R595insREY)	10.26±0.39 [a]
FLT3 (ITD)-NPOS	24.06±1.02 [a]
FLT3 (ITD)-W51	18.23±0.88 [a]
FLT3 (R595_E596insEY)	6.867±0.92 [a]
FLT3 (Y591-V592insVDFREYEYD)	17.72±1.8 [a]
FLT3 (D835V)	7.3±1.2 [b]
FLT3 (ITD)-D835V	160±8 [b]
FLT3 (ITD)-F691L	90±6 [b]

[a] IC_{50} (nM) value in the presence of 10 μM ATP, n = 3 (± SD); [b] *K*d value (nM), n = 3 (± SD).

Table 7. Antiproliferative effects of compound **46** against a panel of FLT3 mutants transformed BaF3 cells [a].

Cell line	IC_{50} (μM)	
	Cpd. **46**	sorafenib
BaF3	9.197±0.293	7.997±0.221
BaF3-FLT3 (ITD)	0.107±0.006	0.006±0.001
BaF3-FLT3 (ITD-D835V)	0.146±0.009	1.454±0.028
BaF3-FLT3 (ITD-F691L)	0.532±0.021	1.348±0.021
BaF3-FLT3 (D835V)	0.211±0.004	1.112±0.032

[a] All IC_{50} values were obtained by triple testing (± SD).

Binding mode simulation of compound 46. We simulated the binding modes of compound **46** with FLT3, FMS and c-kit using induce-fit docking module, and the corresponding results were analyzed using pose view module in Schrödinger software. As presented in **Figure 6A**, two hydrogen bonds formed between the amino moiety of

compound **46** and residue Cys694 of FLT3, and the pyrazole moiety and Glu692, respectively. And the π-cation and π-π interactions formed between compound **46** and Lys614 and Phe691, respectively. An unfavored close contact formed between the pyrazole moiety and backbone NH of Cys694. For FMS and c-kit (**Figure 6B** and **6C**), compound **46** bound to the proteins more deeply in ATP site, perhaps due to the smaller size of their gatekeeper residues Thr663 and Thr623, respectively, compared with Phe691 of FLT3. Hydrogen bonds also formed between compound **46** and the residues in the hinge region of those two kinases; instead, the π-cation and π-π interactions did not form for compound **46**. Furthermore, more unfavorable close contacts emerged when compound **46** interacted with FMS and c-kit. For example, the 1-methylpiperidine moiety may clashed with Lys586 of FMS and Lys593 of c-kit, respectively. It was speculated that the larger amount of the close contacts and the lack of π-π interactions may contributed to the weaker inhibitory activities of compound **46** against FMS and c-kit.

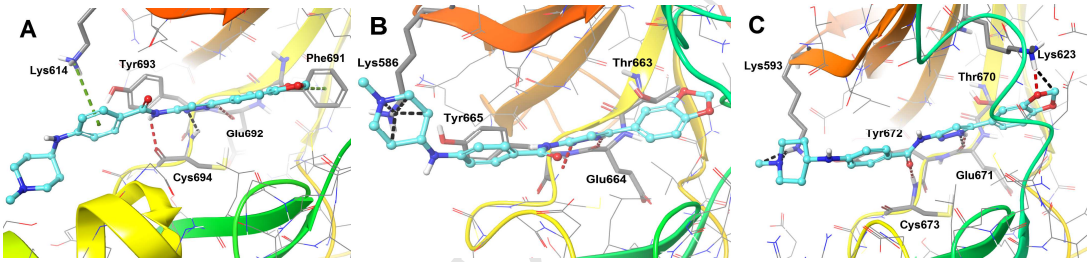

Figure 6. Proposed binding mode of compound **46** with FLT3 homology model (A), FMS (B) and c-kit (C) from molecular docking simulations. Red dash line represents hydrogen bond; green dash line represents π-π interaction or π-cation interaction; black dash line represents the close contact of atoms. Carbon atoms of the residues and the ligand are shown in grey and cyan color, respectively. PDB code for FMS and c-kit crystals: 2I1M and 3G0E.

Cell growth inhibition of compound 46 against other cell lines. Proliferative inhibitory efficacy of compound **46** against other leukemia cell lines and histologically different cell lines was showed in **Table 8**. Only leukemia cell line Molm-13 was sensitive to this compound (IC_{50} = 33.2 nM), which also expressed FLT3-ITD. The other leukemia and solid tumor cell lines, which either expressed wild-type FLT3 or lack expression of FLT3, were resistant to compound **46**. This indicated that anti-growth effect of compound **46** against MV4-11 and Molm-13 cells were dependent on the expression of FLT3-ITD in cells. We also investigated *in vitro* antitumor of **46** against more tumor cell lines by performing the NCI-60 panel screen. As data shown in **Table S4**, most screened tumor cell lines exhibited weak sensitivity to compound **46** even at a high concentration of 10 μM, further suggesting its

selectivity of FLT3-ITD expressing cells.

Table 8. Antiproliferative activity of compound **46** against a variety of cell lines [a].

Cancer type	Cell line	FLT3 status	Inhibition % (1 μM) / IC_{50} (nM)
Breast Cancer	MCF-7	unknown	9.2±1.4 / - [b]
Colorectal	HT-29	unknown	-13.5±1.9 / -
Liver Cancer	Hep G2	unknown	4.3±1.3 / -
Kidney Cancer	ACHN	unknown	-8.3±1.1 / -
Lung Cancer	A-549	unknown	-2.9±0.9 / -
Ovarian Cancer	SK-OV-3	unknown	18.8±1.7 / -
Pancreatic Cancer	BxPC-3	unknown	2.6±0.5 / -
Prostate Cancer	PC-3	unknown	1.5±0.2 / -
Stomach Cancer	MKN-45	unknown	24.1±1.4 / -
Glioblastoma	U251	unknown	1.3±0.2 / -
Esophageal	KYSE-520	unknown	-0.2±0.1 / -
Leukemia	K-562	FLT3-null	-14.9±1.1 / -
Leukemia	HL-60	WT/low	1.6±0.2 / -
Leukemia	Molm-13	ITD	90.3±2.9 / 33.2±4.6
Myeloma	RPMI 8226	unknown	46.0±1.9 / 3795±304
lymphoma	OCI-LY19	unknown	28.7±2.1 / -

[a] Data from triple testing (± SD); [b] Not determined.

Cellular mode of action of compound 46. We analyzed the phosphorylation levels of FLT3, STAT5, ERK and AKT in MV4-11 cells after treated with compound **46** at various concentrations. As shown in **Figure 7**, compound **46** decreased the phosphorylation of FLT3 and its downstream signaling proteins in a dose-dependent manner, suggesting compound **46** could interfere the transduction of FLT3 signal pathway in MV4-11 cells.

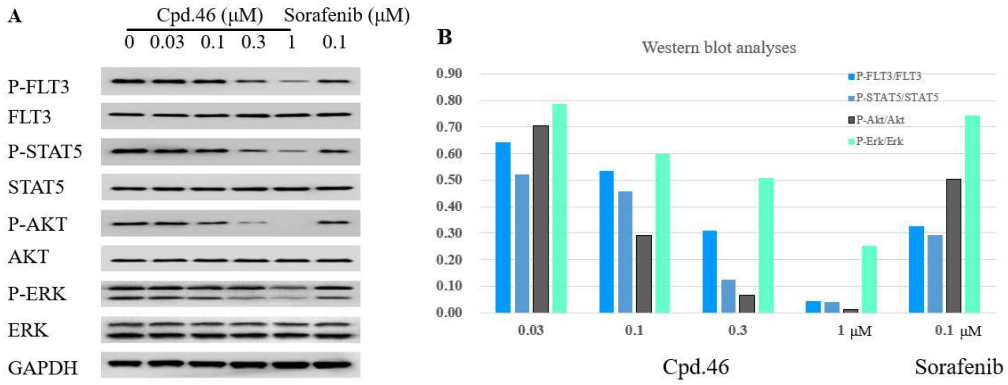

Figure 7. Western blotting analysis of compound **46**. (A) MV4-11 cells were treated with

compound **46** or sorafenib for 24 h; (B) Immunoblotting quantification of P-FLT3, P-STAT5, P-AKT, and P-ERK, respectively. All bands were quantified and normalized by GAPDH.

***In vitro* and *in vivo* PK evaluation.** The metabolic stability of compound **40** and **46** was firstly evaluated by human and rat liver microsomes assay *in vitro*. As the data shown (**Table 9**), compound **40** was metabolically stable in both human and rat liver microsomes. In comparison, compound **46** was more stable in human liver microsomes than in that of rat. Then, PK properties of compound **46** in rats following intravenous and oral administration were studied (**Table 10**). Upon oral administration, the bioavailability was only 22.8%. Upon intravenous administration, a higher C_{max} was observed, which may be beneficial to achieve the antitumor efficacy *in vivo*. Hence, the intravenous administration was selected to evaluate *in vivo* antitumor effect of compound **46**, and the dosing frequency was set as twice per day to offset its shorter $T_{1/2}$. To assist the determination of safe dosage of compound **46** *in vivo*, we investigated its maximum tolerated dose in healthy SPFICR rats. The result showed that the rats were tolerable to dosage up to 200 mg/kg followed the intravenous administration.

Table 9. Pharmacokinetics of compound **40** and **46** in human and rat liver microsomes.

Compound	Liver microsomes	$T_{1/2}$ [a] (min)	CLint [b] (μL/min/mg protein)
40	human	59.8±7.8	23.2±1.1
	rat	41.3±4.2	33.6±0.9
46	human	117±8	11. 8±0.6
	rat	8.27±1.3	168±5

[a] $T_{1/2}$ is half life; [b] C_{Lint} is the intrinsic clearance (± SD).

Table 10. Pharmacokinetics of compound **46** in SD rats. [a]

Parameter	iv (1 mg/kg)	po (5 mg/kg)
$T_{1/2}$ (h)	1.96 ± 0.71	3.07 ± 2.58
C_{max} (ng/mL)	205.37 ± 11.91	27.00 ± 5.36
T_{max} (h)		2.83 ±2.02
$AUC_{(0-t)}$ (h*ng/mL)	152.11 ± 38.96	173.18 ± 29.52
$AUC_{(0-\infty)}$ (h*ng/mL)	160.58 ± 46.35	193.66 ± 40.06
$MRT_{(0-t)}$ (h)	2.75 ± 2.13	5.90 ± 1.96
V_z (L/kg)	18.19 ± 6.58	105.05 ± 81.04
Cl_z (L/h/kg)	6.63 ± 2.09	26.68 ± 6.27

F (%)	22.77 ± 3.88

[a]All testing data were obtained from three independent mice (± SD).

***In vivo* effects of compound 46 in MV4-11 tumor xenografts.** The *in vivo* antitumor efficacy of compound **46** was evaluated in MV4-11 cells inoculated xenograft mouse model, in which a FLT3 inhibitor, sorafenib, was used as the positive control. In addition, compound **40** was tested simultaneously to compare with compound **46**. As data shown in **Figure 8**, *in vivo* tumor inhibition of sorafenib in MV4-11 xenograft mouse model [33] was reproduced, suggesting the results of this experiment was reliable. The 14-day administration of compound **46** and **40** caused almost no body weight loss compared with sorafenib (**Figure 8A**), indicating good tolerance of mice to both compounds. The injections of compound **46** at dosage of 20 and 40 mg/kg twice per day inhibited tumor progression significantly, and its antitumor activity was dose dependent (**Figure 8B**). The antitumor efficacy of 20 mg/kg **46** was comparable to that of sorafenib in terms of inhibitory rate (IR) and rate of relative tumor growth (T/C%) (**Figure 8B** and **8D**), which indicated that **46** showed similar performance with sorafenib in the same total daily dose. The 40 mg/kg **46** produced a T/C% of 8.01% (**Figure 8B**) and a significant IR of 94.65% in tumor weight **(Figure 8D**), which were moderately better than those values of sorafenib. However, the increment of antitumor efficacy for **46** was moderate when its daily dose was doubled. For compound **40**, the IR (81.14%) was weaker than compound **46** at the same dosage, which was consistent with its weaker inhibitory activity against MV4-11 cells *in vitro*.

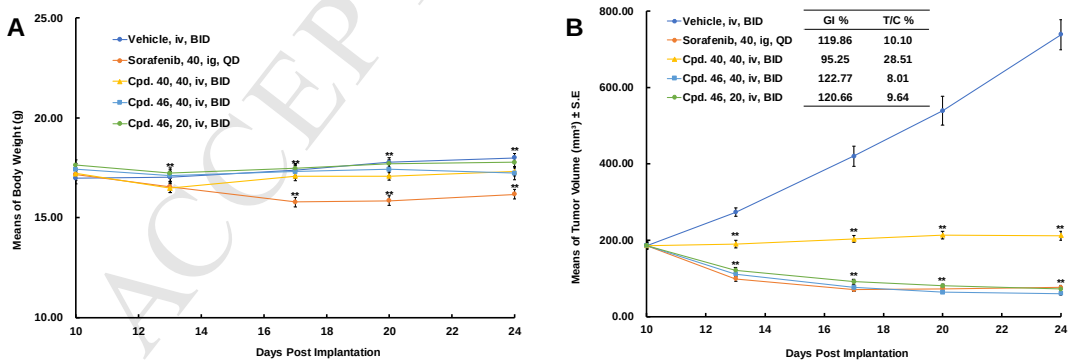

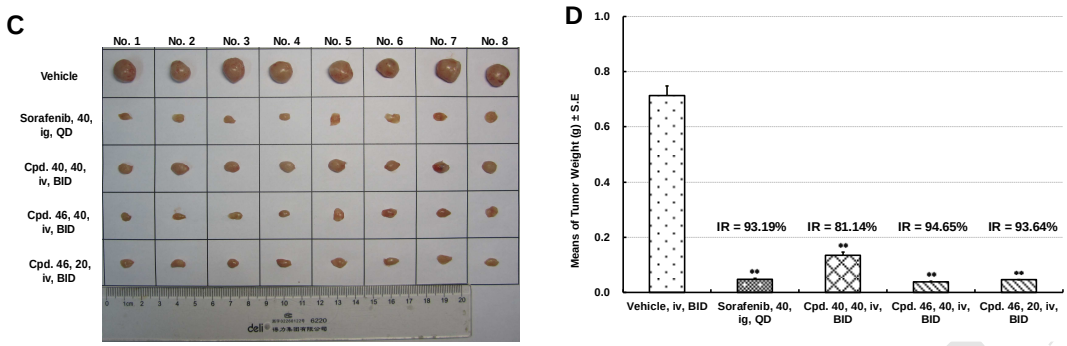

Figure 8. (A) Means of body weights for compound **40**, **46** and sorafenib mice groups and vehicle group in an *in vivo* MV4-11 xenograft model (n = 8). (B) Antitumor efficacy of compound **40**, **46** and sorafenib in an MV4-11 xenograft model (n = 8). (C) Comparison of the final means tumor volume in each group after 14-day treatment period with compound **40**, **46** and sorafenib. (D) The means of tumor weight and inhibition rate for compound **40**, **46** and sorafenib mice groups in an MV4-11 xenograft model (n = 8). ** $P < 0.01$.

To further characterize *in vivo* biological effects of compound **46**, the immunohistochemistry stain assays were performed in the tumor tissues after test compound treatment. **Figure 9A** showed that compound **46** induced apoptosis of tumor cells and inhibited cell proliferation at both dosages, respectively; while tumor cells from vehicle-treated animals had a high proliferative index. Besides, phosphorylation of STAT5 was blocked intensely by compound **46** (**Figure 9A**), which demonstrated the on-target effect of compound **46** *in vivo*. Nevertheless, hematoxylin and eosin (HE) staining results of the viscera of mice indicated that compound **46** were not toxic to normal cells from heart, liver, spleen, lung and kidney as compared with the HE staining results of vehicle groups (**Figure 9B**).

ACCEPTED MANUSCRIPT

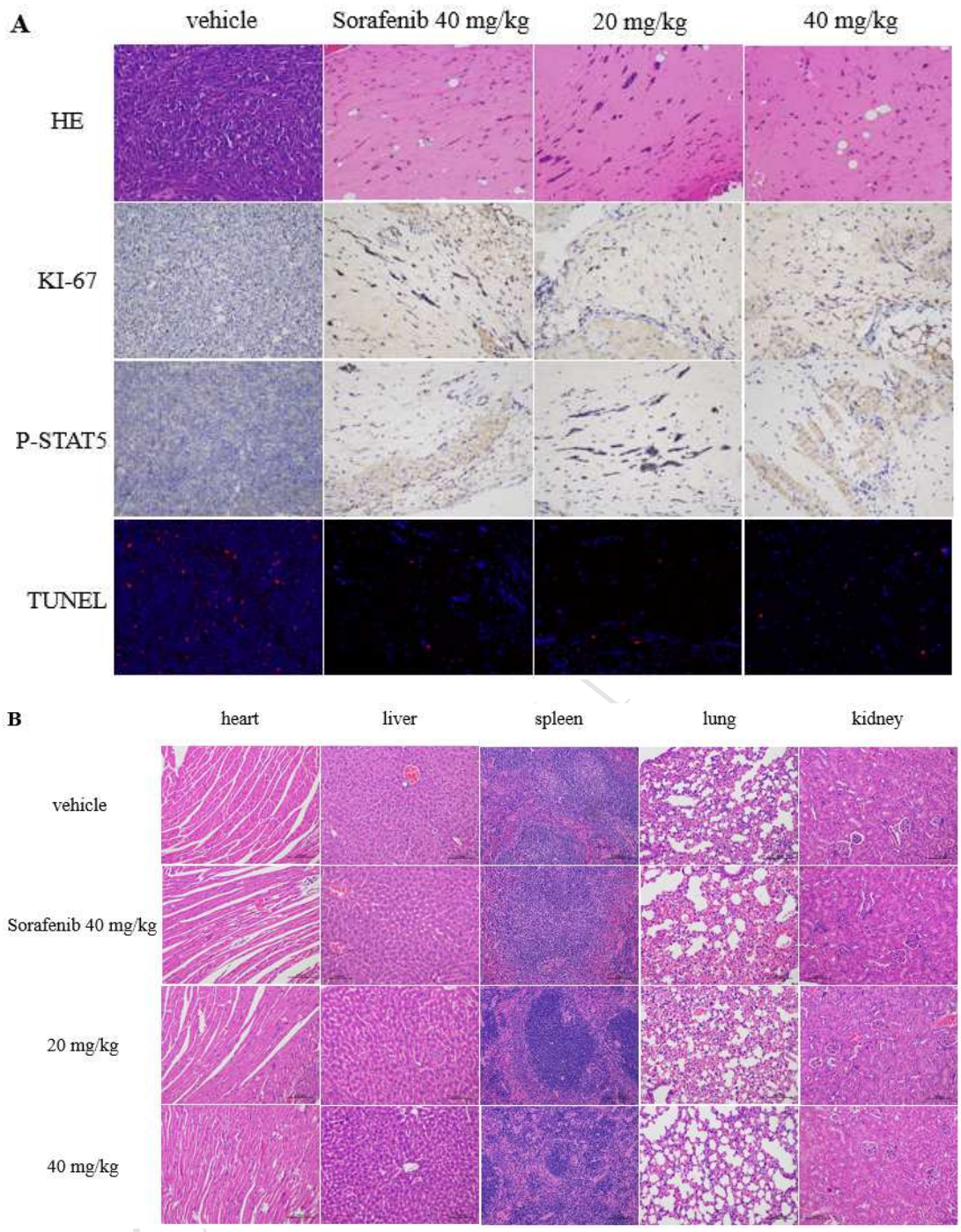

Figure 9. (A) Representative micrographs of hematoxylin and eosin (HE), KI-67, P-STAT5 and TUNEL staining of tumor tissues of **46** treated groups in comparison with the vehicle and sorafenib group. (B) Representative micrographs of hematoxylin and eosin (HE) staining of normal tissues of **46** treated groups in comparison with the vehicle and sorafenib group.

Conclusion

Initiated from our hit compound from virtual screening, a series of FLT3-ITD inhibitors were investigated to improve efficacy against MV4-11 cells that harbored FLT3-ITD mutation, from which we discovered new FLT3 inhibitors with stronger

selectivity than **FN-1501**. The representative compound (**46**) showed potent cellular efficacy and specificity against MV4-11 cells, consistently with its high selectivity against FLT3-ITD over the structurally similar c-kit and FMS kinases. Meanwhile, this compound also displayed inhibitory activities against some concurrent FLT3-ITD-TKD mutants biochemically and in transformed BaF3 cells. Further, the suppression of FLT3 signal pathway by compound **46** was confirmed in MV4-11 cells both *in vitro* and *in vivo*. Compound **46** was well tolerated to mice at dosage up to 200 mg/kg followed the intravenous administration. Furthermore, significant antitumor efficacy was observed for compound **46** in MV4-11-xenograft model with IR of 94.7% and T/C% of 8% at dosage of 40 mg/kg; meanwhile it caused little decrease in mice body weight and showed no obvious toxicity to the viscera of treated mice, indicating its good safety profile. In all, compound **46** represented a potential drug candidate for AML driven by FLT3-ITD mutation.

EXPERMENTAL SECTION

Reagents and General Methods. Unless otherwise specified, reagents were purchased from commercial suppliers and used without further purification. Melting points were determined by X-4 digital display micro-melting point apparatus (Beijing Tech Instrument Co., Ltd.); NMR spectra were recorded on Bruker AVANCE AV-600 spectrometer (600 MHz for ^{1}H, 151 MHz for ^{13}C) or AVANCE AV-500 spectrometer (500 MHz for ^{1}H, 126 MHz for ^{13}C) or AVANCE AV-400 spectrometer (400 MHz for ^{1}H, 101 MHz for ^{13}C) or Bruker AVANCE AV-300 spectrometer (300 MHz for ^{1}H, 75 MHz for ^{13}C); Mass spectra were obtained on the Agilent 1100 LC / MSD mass spectrometer (Agilent, USA) or Q-tofmicro MS (micromass company). All reactions were monitored by TLC (Merck Kieselgel GF254) and spots were visualized with UV light or iodine. The purity of biologically evaluated compounds was >95% as determined by HPLC (Agilent Technologies). Ten μL of the solution was injected on a column (150 mm × 4.6 mm; 5 μm; Symmetry C18, ZORBAX SB-C18 PN883975-902). The column was kept in a thermostat at 25 °C. Water and methanol were used as the mobile phase at flow rate of 1 mL·min^{-1}.

Procedure for the synthesis of compound 1. To a stirring solution of 4-bromo-2-thiophenecarboxylic acid (3 g, 14.5 mmol) in methanol (25 mL) was added thionyl chloride (1.74 g, 14.5 mmol). Reaction mixture was heated to reflux and stirred for 6 h. Upon completion, the residue was taken up in ice water (60 mL). The pH was adjusted to 9-10 with saturated sodium carbonate solution. The aqueous phase was extracted with ethyl acetate (40 mL × 3). The combined organic phase was washed twice with saturated brine (20 mL × 2) and dried over anhydrous $MgSO_4$. After filtering out $MgSO_4$, the solvent of filtrate was removed in vacuo to

afford crude product of title compound as a pale-yellow oil which was used for next step directly. Yield: 98%; ^{1}H NMR (300 MHz, $CDCl_3$) δ: 7.69 (s, 1H), 7.45 (s, 1H), 3.90 (s, 3H). MS (m/z): $[M+H]^+$ 221.0, 223.0.

Procedure for the synthesis of compound 2. In a sealed tube, compound **1** (5.00 g, 22.6 mmol) was dissolved in anhydrous DMF (5 mL) followed by the addition of cuprous cyanide (6.08 g, 67.9 mmol) and potassium iodide (0.01 g, 0.06 mmol) under an argon atmosphere. Reaction mixture was heated at 160 °C for 10 h. After this period, the reaction was quenched with a mixed solution of ammonia and ice water (v / v = 1 : 3, 50 mL). The precipitate was filtered out and rinsed with ethyl acetate. The filtrate was` extracted with ethyl acetate (40 mL × 3). The combined organic phase was washed twice with saturated brine (30 mL × 2) and dried over anhydrous $MgSO_4$. The solvent was removed in vacuo and the residue was purified by silica gel column chromatography (PE : EA = 20 : 1) to give title compound as a white solid. Yield: 79%; mp: 107-109 °C. ^{1}H NMR (300 MHz, $CDCl_3$) δ: 8.09 (s, 1H), 7.93 (s, 1H), 3.93 (s, 3H). MS (m/z): $[M+H]^+$ 168.1.

Procedure for the synthesis of compound 3. To a stirring solution of compound **2** (1.67 g, 10 mmol) in anhydrous ethanol (25mL) was added hydrazine hydrate (1.19 g, 10 mmol). Reaction was stirred at 45 °C for 10 h. The solvent was removed in vacuo to afford the pale-yellow solid, which was recrystallized with 95% ethanol to give title compound as a white solid. Yield: 87%; mp: 162-164 °C; ^{1}H NMR (300 MHz, DMSO-d_6) δ: 10.00 (s, 1H), 8.73 (d, J = 1.3 Hz, 1H), 7.99 (d, J = 1.3 Hz, 1H), 4.58 (s, 2H). MS (m/z): $[M+H]^+$ 168.21, MS (m/z): $[M-H]^-$ 166.30.

General procedure for the synthesis of compound 4a-4b. To a stirring solution of 4-fluoronitrobenzene (1.41 g, 10.00 mmol) in anhydrous DMF (25 mL) were added 1-methylpiperazine (1.01 g, 10.00 mmol) and triethylamine (1.01 g, 10.00 mmol). Reaction was stirred at r.t. for 24 h. Upon completion, the residue was taken up in ice water (60 mL). The pH was adjusted to 8 with saturated sodium carbonate solution, and the aqueous phase was extracted with ethyl acetate (40 mL × 3). The combined organic phase was washed twice with saturated brine (30 mL × 2) and dried over anhydrous $MgSO_4$. After filtering out $MgSO_4$, the solvent of filtrate was removed in vacuo and the residue was purified by silica gel column chromatography (PE : EA = 1 : 1) to afford compound **4a** as an orange solid. Yield: 85%. mp: 35-38 °C; ^{1}H NMR (300 MHz, DMSO-d_6) δ: 8.05 (d, J = 9.5 Hz, 2H), 7.03 (d, J = 9.5 Hz, 2H), 3.54−3.37 (m, 4H), 2.47−2.38 (m, 4H), 2.22 (s, 3H). MS (m/z): $[M+H]^+$ 222.3.

1-Methyl-4-(3-nitrophenyl)piperazine (4b)

Yellow solid was afforded as the crude product which was used in next step without further purification. MS (m/z): $[M+H]^+$ 222.2.

General procedure for the synthesis of compound 4c-4g. To a stirring solution of 4-nitrobenzoic acid (1.67 g, 10 mmol) in anhydrous DMF (30 mL) were added 3-morpholinylpropylamine (1.44 g, 10 mmol), HATU (7.6 g, 20 mmol) and *N*, *N*-diisopropylethylamine (3 mL, 4 mmol). Reaction mixture was stirred at 35 ℃ for 4 h. Upon completion, the residue was taken up in ice water (60 mL). The aqueous phase was extracted with ethyl acetate (50 mL × 3). The combined organic phase was washed twice with saturated brine (20 mL × 2) and dried over anhydrous $MgSO_4$. After filtration, the solvent of filtrate was removed in vacuo, and the residue was purified by silica gel column chromatography (DCM : MeOH : Et_3N = 300 : 1 : 1) to afford compound **4d** as a white solid; Yield: 70%; mp: 182-184 °C; ^{1}H NMR (400 MHz, DMSO-d_6) δ: 8.89 (s, 1H), 8.44−8.21 (m, 2H), 8.17−7.90 (m, 2H), 3.67 (s, 4H), 2.75 (s, 4H), 1.81 (s, 2H). MS (m/z): $[M+H]^+$ 294.2.

(4-Methylpiperazin-1-yl)(4-nitrophenyl)methanone (4c)

White solid was afforded as the crude product which was used in next step without further purification. MS (m/z): $[M+H]^+$ 250.2.

***N*-(3-(diethylamino)propyl)-4-nitrobenzamide (4e)**

White solid was afforded as the crude product which was used in next step without further purification. MS (m/z): $[M+H]^+$ 280.1.

(4-Methylpiperazin-1-yl)(3-nitrophenyl)methanone (4f)

White solid was afforded as the crude product which was used in next step without further purification. MS (m/z): $[M+H]^+$ 250.3.

***N*-(1-methylpiperidin-4-yl)-4-nitrobenzamide (4g)**

White solid was afforded as the crude product which was used in next step without further purification. MS (m/z): $[M+H]^+$ 264.3.

General procedure for the synthesis of compound 5a-5g. To a stirring solution of compound **4a** (1.2 g, 4.77 mmol) in 70% ethanol (20 mL) were added ammonium chloride (1.28 g, 23.85 mmol) and reduced iron powder (0.8 g, 14.31 mmol). The reaction was refluxed for 5 h. Upon completion, the mixture was filtered while hot and rinsed with ethyl acetate. The solvent was removed in vacuo, and the residue was purified by silica gel column chromatography (PE : EA = 1 : 2) to afford compound **5a** as an orange solid. Yield: 97%; mp: 108-110 °C; ^{1}H NMR (300 MHz, DMSO-d_6) δ 6.67 (d, J = 8.8 Hz, 2H), 6.48 (d, J = 8.8 Hz, 2H), 4.53 (s, 2H), 2.92−2.84 (m, 4H), 2.46−2.36 (m, 4H), 2.19 (s, 3H). MS (m/z): $[M+H]^+$ 192.3.

3-(4-Methylpiperazin-1-yl)aniline (5b)

Brown oil was afforded as the crude product which was used in next step without further purification. MS (m/z): $[M+H]^+$ 192.1.

(4-Aminophenyl)(4-methylpiperazin-1-yl)methanone (5c)

White solid was afforded as the crude product which was used in next step without further purification. MS (m/z): $[M+H]^+$ 220.3.

4-Amino-*N*-(3-morpholinopropyl)benzamide (5d)

White solid was afforded as the crude product which was used in next step without further purification. MS (m/z): $[M+H]^+$ 264.2.

4-Amino-*N*-(3-(diethylamino)propyl)benzamide (5e)

White solid was afforded as the crude product which was used in next step without further purification. MS (m/z): $[M+H]^+$ 250.2.

(3-Aminophenyl)(4-methylpiperazin-1-yl)methanone (5f)

Light yellow solid was afforded as the crude product which was used in next step without further purification. MS (m/z): $[M+H]^+$ 220.3.

4-Amino-*N*-(1-methylpiperidin-4-yl)benzamide (5g)

Light yellow solid was afforded as the crude product which was used in next step without further purification. MS (m/z): $[M+H]^+$ 234.3.

General procedure for the synthesis of compound 6a-6g. An aqueous solution of sodium bicarbonate (0.57 g, 6.78 mmol) (20 mL) was stirred at r.t. for 10 min, and then compound **5a** (0.50 g, 2.26 mmol) in dichloromethane (10 mL) was added under ice-cooling. Thiophosgene (0.39 g, 3.39 mmol) in dichloromethane solution (5 mL) was added dropwise for 0.5 h. Reaction was stirred under ice-cooling for 6 h. The aqueous phase was extracted with dichloromethane (20 mL × 3). The combined organic phase was washed twice with saturated brine (20 mL × 2) and dried over anhydrous $MgSO_4$. After filtration, the solvent of filtrate was removed in vacuo, and the residue was purified by silica gel column chromatography (DCM : MeOH = 100 : 1) to afford compound **6a** as a pale-yellow solid; Yield: 63%; mp: 94-96 °C; ^{1}H NMR (300 MHz, DMSO-d_6) δ: 7.27 (d, J = 9.0 Hz, 2H), 6.95 (d, J = 9.1 Hz, 2H), 3.24−3.15 (m, 4H), 2.49−2.39 (m, 4H), 2.23 (s, 3H). MS (m/z): $[M+H]^+$ 234.1.

1-(3-Isothiocyanatophenyl)-4-methylpiperazine (6b)

Brown oil was afforded as the crude product which was used in next step without further purification. MS (m/z): $[M+H]^+$ 234.1, MS (m/z): $[M-H]^-$ 232.1.

(4-Isothiocyanatophenyl)(4-methylpiperazin-1-yl)methanone (6c)

White solid was afforded as the crude product which was used in next step without further purification. MS (m/z): $[M+H]^+$ 262.1, MS (m/z): $[M-H]^-$ 260.1.

4-Isothiocyanato-*N*-(3-morpholinopropyl)benzamide (6d)

White solid was afforded as the crude product which was used in next step without further purification. MS (m/z): $[M+H]^+$ 306.1.

***N*-(3-(diethylamino)propyl)-4-isothiocyanatobenzamide (6e)**

White solid was afforded as the crude product which was used in next step without further purification. MS (m/z): $[M+H]^+$ 292.4.

(3-Isothiocyanatophenyl)(4-methylpiperazin-1-yl)methanone (6f)

White solid was afforded as the crude product which was used in next step without further purification. MS (m/z): $[M+H]^+$ 262.1.

4-Isothiocyanato-*N*-(1-methylpiperidin-4-yl)benzamide (6g)

White solid was afforded as the crude product which was used in next step without further purification. MS (m/z): $[M+H]^+$ 276.4.

General procedure for the synthesis of compound 7a-7g. To a stirring solution of compound **3** (0.17 g, 1 mmol) in anhydrous ethanol (10 mL) were added compound **6a** (0.26 g, 1.1 mmol) and pyridine (0.79 mg, 0.01 mmol). Reaction mixture was refluxed for 1 h. Upon completion, the solvent was removed in vacuo, and the residue was Recrystallized with 95% ethanol to afford compound **7a** as a pale-yellow solid which was used in next step directly. Yield: 52%; mp: 192-194 °C; ^{1}H NMR (300 MHz, DMSO-d_6) δ: 12.52 (s, 1H), 10.60 (s, 1H), 10.39 (s, 1H), 8.28 (s, 1H), 8.07 (s, 1H), 6.66−6.64 (m, 2H), 6.30−6.28 (m, 2H), 3.31−2.43 (m, 8H), 2.21 (s, 3H). MS (m/z): $[M+H]^+$ 401.1, MS (m/z): $[M-H]^-$ 399.1.

General procedure for the synthesis of compound 8-14.

5-(5-((4-(4-Methylpiperazin-1-yl)phenyl)amino)-1,3,4-oxadiazol-2-yl)thiophene-3-carbonitril e (8). To a stirring solution of compound **7a** (0.4 g, 1 mmol) in anhydrous ethanol (15 mL) was added mercury acetate (0.35 g, 1.1 mmol). Reaction mixture was heated to reflux and stirred for 3 h. Upon completion, the mixture was filtered and rinsed with methanol. The solvent was removed in vacuo, and the residue was purified by silica gel column chromatography (DCM : MeOH : TEA = 40 : 2 : 1) to afford title compound as a white solid. Yield: 26%; mp: 255-257 °C; ^{1}H NMR (300 MHz, DMSO-d_6) δ: 10.50 (s, 1H), 8.77−8.76 (m, 1H), 7.97−7.96 (m, 1H), 7.46−7.43 (m, 2H), 6.97−6.94 (m, 2H), 3.09−3.06 (m, 4H), 2.51−2.46 (m, 4H), 2.24 (s, 3H). ^{13}C NMR (151 MHz, DMSO-d_6) δ: 60.53 (s), 153.04 (s), 146.70 (s), 140.66 (s), 131.08 (s), 128.90 (s), 127.79 (s), 118.87 (s), 116.95 (s), 115.01 (s), 110.94 (s), 63.00 (s), 61.18 (s), 54.51 (s), 52.45 (s), 29.66 (s), 7.65 (s). HRMS-EI m/z $[M+H]^+$ calcd for $C_{18}H_{19}N_6OS$: 367.1341, found: 367.1319.

5-(5-((3-(4-Methylpiperazin-1-yl)phenyl)amino)-1,3,4-oxadiazol-2-yl)thiophene-3-carbonitril e (9). The preparation of compound **9** was similar with that of compound **8** to afford title compound as a yellow solid. Yield: 42%; mp: 250-251 °C; ^{1}H NMR (300 MHz, DMSO-d_6) δ: 10.64 (s, 1H), 8.79−8.78 (m, 1H), 7.97−7.96 (m, 1H), 7.28−6.59 (m, 4H), 3.15-3.12 (m, 4H), 2.50−2.45 (m, 4H), 2.23 (s, 3H). HRMS-EI m/z $[M+H]^+$ calcd for $C_{18}H_{19}N_6OS$: 367.1341, found: 367.1311.

5-(5-((4-(4-Methylpiperazine-1-carbonyl)phenyl)amino)-1,3,4-oxadiazol-2-yl)thiophene-3-car

bonitrile (10). The preparation of compound **10** was similar with that of compound **8** to afford title compound as a yellow solid. Yield: 42%; mp: 292-293 °C; ^{1}H NMR (300 MHz, DMSO-d_6) δ: 11.26 (s, 1H), 8.83 (s, 1H), 8.04 (s, 1H), 7.69 (d, J = 8.0 Hz, 2H), 7.42 (d, J = 8.0 Hz, 2H), 3.56 (m, 4H), 2.33 (m, 2H), 2.20 (s, 3H). ^{13}C NMR (151 MHz, DMSO-d_6) δ: 169.26 (s), 160.06 (s), 153.55 (s), 141.07 (s), 139.98 (s), 129.40 (s), 128.94 (s), 127.52 (s), 117.18 (s), 114.97 (s), 110.96 (s), 45.97 (s), 0.58 (s). HRMS-EI m/z $[M+H]^+$ calcd for $C_{19}H_{19}N_6O_2S$: 395.1290, found: 395.1276.

5-(5-((3-(4-Methylpiperazine-1-carbonyl)phenyl)amino)-1,3,4-oxadiazol-2-yl)thiophene-3-carbonitrile (11). The preparation of compound **11** was similar with that of compound **8** to afford title compound as a white solid. Yield: 52%; mp: 261-263 °C; ^{1}H NMR (300 MHz, DMSO-d_6) δ: 10.99 (s, 1H), 8.80−8.79 (m, 1H), 8.02−8.01 (m, 1H), 7.66−7.01(m, 4H), 3.60−3.42 (m, 4H), 3.32−3.20 (m, 2H), 2.20 (s, 3H). HRMS-EI m/z $[M+H]^+$ calcd for $C_{19}H_{19}N_6O_2S$: 395.1290, found: 395.1268.

4-((5-(4-Cyanothiophen-2-yl)-1,3,4-oxadiazol-2-yl)amino)-*N*-(1-methylpiperidin-4-yl)benzamide (12). The preparation of compound **12** was similar with that of compound **8** to afford title compound as a white solid. Yield: 47%; mp: 266-268 °C; ^{1}H NMR (300 MHz, DMSO-d_6) δ: 11.10 (s, 1H), 8.81−8.80 (m, 1H), 8.12−8.09 (m, 1H), 8.03−8.01 (m, 1H), 7.89−7.86 (m, 2H), 7.66−7.63 (m, 2H), 3.75−3.67 (m, 1H), 2.79−2.75 (m, 2H), 2.17 (s, 3H), 1.98−1.91 (m, 2H), 1.77−1.74 (m, 2H), 1.64−1.52 (m, 2H). ^{13}C NMR (151 MHz, DMSO-d_6) δ: 172.61 (s), 165.60 (s), 159.96 (s), 153.59 (s), 141.22 (s), 141.00 (s), 129.37 (s), 129.07 (s), 128.46 (s), 127.51 (s), 116.79 (s), 114.95 (s), 111.00 (s), 54.24 (s), 52.46 (s), 46.10 (s), 45.29 (s), 31.00 (s), 21.66 (s), 7.66 (s). HRMS-EI m/z $[M+H]^+$ calcd for $C_{20}H_{21}N_6O_2S$: 409.1447, found: 409.1449.

4-((5-(4-Cyanothiophen-2-yl)-1,3,4-oxadiazol-2-yl)amino)-*N*-(3-morpholinopropyl)benzamide (13). The preparation of compound **13** was similar with that of compound **8** to afford title compound as a white solid. Yield: 51%; mp: 279-281 °C; ^{1}H NMR (300 MHz, DMSO-d_6) δ: 11.11 (s, 1H), 8.81−8.80 (m, 1H), 8.37−8.34 (m, 1H), 8.03−8.01 (m, 1H), 7.88−7.85 (m, 2H), 7.66−7.63 (m, 2H), 3.58−3.55 (m, 4H), 3.31−3.25 (m, 2H), 2.34−2.29 (m, 6H), 1.72 (m, 2H). ^{13}C NMR (151 MHz, DMSO-d_6) δ: 165.99 (s), 159.99 (s), 153.60 (s), 141.18 (s), 141.04 (s), 129.41 (s), 128.86 (s), 128.56 (s), 127.52 (s), 116.88 (s), 114.96 (s), 110.99 (s), 56.59 (s), 55.39 (s), 53.81 (s), 40.47 (s), 38.17 (s), 29.65 (s), 26.50 (s). HRMS-EI m/z $[M+H]^+$ calcd for $C_{20}H_{21}N_6O_2S$: 439.1552, found: 439.1519.

4-((5-(4-Cyanothiophen-2-yl)-1,3,4-oxadiazol-2-yl)amino)-*N*-(3-(diethylamino)propyl)benzamide (14). The preparation of compound **14** was similar with that of compound **8** to afford title compound as a white solid. Yield: 52%; mp: 254-255 °C; ^{1}H NMR (300 MHz, DMSO-d_6) δ: 8.81−8.80 (m, 1H), 8.41−8.37 (m, 1H), 8.02−8.79 (m, 1H), 7.87−7.83 (m, 2H), 7.65−7.62 (m, 2H), 3.30−3.24 (m, 2H), 2.44−2.40 (m, 6H), 1.66−1.59 (m, 2H), 0.97−0.92 (m, 6H). ^{13}C NMR

(151 MHz, DMSO-d_6) δ: 165.96 (s), 159.98 (s), 153.60 (s), 141.16 (s), 141.01 (s), 129.40 (s), 128.81 (s), 128.59 (s), 127.52 (s), 116.89 (s), 114.96 (s), 111.02 (s), 55.38 (s), 50.53 (s), 46.72 (s), 38.33 (s), 26.76 (s), 11.83 (s). HRMS-EI m/z $[M+H]^+$ calcd for $C_{21}H_{25}N_6O_2S$: 425.1760, found: 425.1745.

General procedure for the synthesis of compound 15-18.

5-(5-((3-(4-Methylpiperazin-1-yl)phenyl)amino)-1,3,4-oxadiazol-2-yl)thiophene-3-carboxamide (15). To a stirring solution of compound **9** (0.125 g, 0.342 mmol) in anhydrous ethanol (4 mL) were added 30% H_2O_2 (0.1 mL) and 6N aqueous NaOH (0.15 mL). Reaction was stirred at 50 °C for 6 h. Upon completion, the mixture was filtered and rinsed with methanol. The solvent was removed in vacuo, and the residue was purified by silica gel column chromatography (DCM : MeOH : TEA = 40 : 2 : 1) to afford title compound as a white solid. Yield: 51%; mp: 255-256 °C; ^{1}H NMR (300 MHz, DMSO-d_6) δ: 10.95 (s, 1H), 8.35−8.34 (m, 1H), 8.03 (s, 1H), 7.93−7.92 (m, 1H), 7.43−7.42 (s, 1H), 7.27−6.60 (m, 4H), 3.15−3.12 (m, 4H), 2.50−2.45 (m, 4H), 2.23 (s, 3H). HRMS-EI m/z $[M+H]^+$ calcd for $C_{18}H_{21}N_6O_2S$: 385.1447, found: 385.1418.

5-(5-((4-(4-Methylpiperazine-1-carbonyl)phenyl)amino)-1,3,4-oxadiazol-2-yl)thiophene-3-carboxamide (16). The preparation of compound **16** was similar with that of compound **15** to afford title compound as a white solid. Yield: 52%; mp: 272-274 °C; ^{1}H NMR (300 MHz, DMSO-d_6) δ: 10.96 (s, 1H), 8.36 (d, 1H), 8.00 (s, 1H), 7.99−7.98 (m, 1H), 7.43 (s, 1H), 7.27−6.60 (m, 4H), 3.48−3.35 (m, 4H), 2.31−2.30 (m, 4H), 1.97 (s, 3H). ^{13}C NMR (151 MHz, DMSO-d_6) δ: 169.25 (s), 163.15 (s), 159.73 (s), 154.39 (s), 140.05 (s), 139.15 (s), 132.90 (s), 129.53 (s), 128.97 (s), 127.98 (s), 125.74 (s), 117.06 (s), 55.38 (s), 54.97 (s), 46.08 (s). HRMS-EI m/z $[M+H]^+$ calcd for $C_{19}H_{21}N_6O_3S$: 413.1396, found: 413.1407.

5-(5-((4-((3-Morpholinopropyl)carbamoyl)phenyl)amino)-1,3,4-oxadiazol-2-yl)thiophene-3-carboxamide (17). The preparation of compound **17** was similar with that of compound **15** to afford title compound as a white solid. Yield: 44%; mp: 278-280 °C; ^{1}H NMR (300 MHz, DMSO-d_6) δ: 11.02 (s, 1H), 8.81−8.79 (m, 2H), 8.02−7.98 (m, 2H), 7.88−7.86 (m, 2H), 7.69−7.67 (m, 2H), 7.44 (s, 1H), 3.59-3.56 (m, 4H), 3.33-3.26 (m, 2H), 2.35-2.31 (m, 6H), 1.72-1.64 (m, 2H). HRMS-EI m/z $[M+H]^+$ calcd for $C_{21}H_{25}N_6O_4S$: 457.1658, found: 457.1637.

5-(5-((4-((3-(Diethylamino)propyl)carbamoyl)phenyl)amino)-1,3,4-oxadiazol-2-yl)thiophene-3-carboxamide (18). The preparation of compound **18** was similar with that of compound **15** to afford title compound as a white solid. Yield: 42%; mp: 272-274 °C; ^{1}H NMR (300 MHz, DMSO-d_6) δ: 11.00 (s, 1H), 8.41-8.36 (m, 2H), 8.00−7.98 (m, 2H), 7.86−7.83 (m, 2H), 7.66−7.63 (m, 2H), 7.43 (s, 1H), 3.26−3.24 (m, 2H), 2.47−2.41 (m, 6H), 1.68−1.59 (m, 2H), 0.97−0.92 (m, 6H). ^{13}C NMR (151 MHz, DMSO-d_6) δ:166.05 (s), 163.15 (s), 159.67 (s), 154.45 (s), 141.33 (s), 139.16 (s), 132.94 (s), 128.83 (s), 128.39 (s), 128.05 (s), 125.70 (s), 116.83 (s), 52.42 (s), 50.28

(s), 46.69 (s) , 38.10 (s), 26.33 (s), 11.31 (s), 7.61 (s), 0.56 (s). HRMS-EI m/z $[M+H]^+$ calcd for $C_{21}H_{27}N_6O_3S$: 443.1865, found: 443.1838.

General procedure for the synthesis of compound 19a-19g. A mixture of 60% NaH (0.12 g, 5 mmol) was added in anhydrous THF (10 mL), followed by the addition of anhydrous CH_3CN (0.21 g, 5 mmol) and compound **2** (0.42 g, 2.5 mmol) in the ice bath. Reaction was heated to reflux and stirred for 6 h. Upon completion, the reaction mixture was taken up in ice water (30 mL) and the pH was adjusted to 5. After filtration, the filtrate was extracted with ethyl acetate (20 mL × 3). The combined organic phase was washed twice with saturated brine (20 mL × 2) and dried over anhydrous $MgSO_4$. Then, $MgSO_4$ was filtered out, and the filtrate was concentrated in vacuo, Followed by recrystallization of the residue to afford compound **19a** as a pale-yellow solid. Yield：52%. mp: 151-153 °C; ^{1}H NMR (600 MHz, DMSO-d_6) δ: 9.01(s, 1H), 8.43 (s, 1H), 4.72 (s, 2H). MS (m/z): $[M+H]^+$ 176. 1.

3-(Benzo[*b*]thiophen-2-yl)-3-oxopropanenitrile (19b)

Light yellow solid. Yield: 73%. mp: 120-121 °C; ^{1}H NMR (300 MHz, DMSO-d_6) δ: 13.51 (s, 0.8H), 8.42−8.11 (m, 1H), 8.11−7.95 (m, 2H), 7.61−7.41 (m, 2H), 4.86 (s, 0.4H). MS (m/z): $[M-H]^-$ 199.9.

3-(Benzo[*d*][1,3]dioxol-5-yl)-3-oxopropanenitrile (19c)

Yellow solid. Yield: 71%. mp: 131-133 °C; ^{1}H NMR (300 MHz, $CDCl_3$) δ: 7.49 (dd, J = 8.2, 1.8 Hz, 1H), 7.40 (d, J = 1.8 Hz, 1H), 6.90 (d, J = 8.2 Hz, 1H), 6.10 (s, 2H), 4.01 (s, 2H). MS (m/z): $[M+H]^+$ 190.2.

3-(2,3-Dihydrobenzo[*b*][1,4]dioxin-6-yl)-3-oxopropanenitrile (19d)

White solid. Yield: 92%. mp: 168-170 °C; ^{1}H NMR (300 MHz, DMSO-d_6) δ: 7.52−7.47 (m, 1H), 7.44−7.43 (m, 1H), 7.03−7.00 (m, 1H), 4.67 (s, 2H), 4.35−4.33 (m, 2H), 4.31−4.29 (m, 2H). MS (m/z): $[M+Na]^+$ 226.0.

3-(2,2-Difluorobenzo[*d*][1,3]dioxol-5-yl)-3-oxopropanenitrile (19e)

Light yellow solid. Yield: 93%. mp: 69-70 °C; ^{1}H NMR (300 MHz, DMSO-d_6) δ: 11.70 (s, 0.09H) 7.97 (d, J = 1.7 Hz, 1H), 7.89 (dd, J = 8.5, 1.8 Hz, 1H), 7.62 (d, J = 8.5 Hz, 1H), 4.76 (s, 1.82H). MS (m/z): $[M-H]^-$ 224.0.

3-(2,3-Dihydrobenzofuran-5-yl)-3-oxopropanenitrile (19f)

Yellow solid. Yield: 95%. mp: 123-124 °C; ^{1}H NMR (300 MHz, $CDCl_3$) δ: 7.83 (q, J = 1.5 Hz, 1H), 7.73 (dd, J = 8.5, 2.0 Hz, 1H), 6.85 (d, J = 8.5 Hz, 1H), 4.69 (d, J = 8.8 Hz, 2H), 3.99 (s, 2H), 3.27 (q, J = 8.8 Hz, 2H). MS (m/z): $[M-H]^-$ 185.9.

3-(3,4-Dimethoxyphenyl)-3-oxopropanenitrile (19g)

Light yellow solid. Yield: 96%. mp: 139-141 °C; ^{1}H NMR (300 MHz, $CDCl_3$) δ: 7.54−7.47 (m, 2H), 6.92 (d, J = 8.9 Hz, 1H), 4.05 (s, 2H), 3.98 (s, 3H), 3.95 (s, 3H). MS (m/z): $[M+H]^+$ 206.1.

General procedure for the synthesis of compound 20 and 21a-21f. To a stirring solution of compound **19a** (0.18 g, 1 mmol) in ethanol (10 mL) was added 80% hydrazine hydrate (0.15 g, 1.5 mmol). Reaction was heated to reflux and stirred for 5 h. Upon completion, the reaction mixture was taken up in ice water (20 mL). The aqueous phase was extracted with ethyl acetate (20 mL × 3). The combined organic phase was washed twice with saturated brine (20 mL × 2) and dried over anhydrous $MgSO_4$. The solvent was removed in vacuo, and the residue was purified by silica gel column chromatography (PE : EA = 2 : 1) to afford compound **20** as white solid. Yield: 47%. mp: 177-179 °C; ^{1}H NMR (600 MHz, DMSO-d_6) δ: 11.66 (s, 1H), 8.36 (s, 1H), 7.61 (s, 1H), 5.66 (s, 1H), 5.19 (s, 2H). MS (m/z): $[M+H]^+$ 191.1.

3-(Benzo[*b*]thiophen-2-yl)-1*H*-pyrazol-5-amine (21a)

Grey solid. Yield: 48%. mp: 169-171 °C; ^{1}H NMR (300 MHz, DMSO-d_6) δ: 7.93−7.83 (m, 1H), 7.82−7.67 (m, 1H), 7.53 (s, 1H), 7.31 (pd, J = 7.2, 1.5 Hz, 2H), 5.73 (s, 1H). MS (m/z): $[M+H]^+$ 216.1.

3-(Benzo[*d*][1,3]dioxol-5-yl)-1*H*-pyrazol-5-amine (21b)

Grey solid. Yield: 65%. mp: 132-134 °C; ^{1}H NMR (300 MHz, DMSO-d_6) δ: 12.82 (s, 1H), 7.67 (s, 1H), 7.39−7.27 (m, 2H), 6.95 (dd, J = 8.1, 2.5 Hz, 1H), 6.62 (d, J = 2.5 Hz, 1H), 6.04 (d, J = 2.6 Hz, 2H). MS (m/z): $[M+H]^+$ 204.2.

3-(2,3-Dihydrobenzo[*b*][1,4]dioxin-6-yl)-1*H*-pyrazol-5-amine (21c)

White solid. Yield: 62%. mp: 173-175 °C; ^{1}H NMR (300 MHz, DMSO-d_6) δ: 11.62 (brs, 1H), 7.13−7.10 (m, 2H), 6.86 (d, J = 8.3 Hz, 1H), 5.65 (s, 1H), 4.70 (s, 2H), 4.24−4.22 (m, 4H). MS (m/z): $[M+H]^+$ 218.1.

3-(2,2-Difluorobenzo[*d*][1,3]dioxol-5-yl)-1*H*-pyrazol-5-amine (21d)

Light pink solid. Yield: 58%. mp: 112-114 °C; ^{1}H NMR (300 MHz, DMSO-d_6) δ: 11.72 (s, 1H), 7.67 (d, J = 3.0 Hz, 1H), 7.51 (dd, J = 8.5, 2.4 Hz, 1H), 7.39 (dt, J = 8.5, 2.4 Hz, 1H), 5.81−5.72 (m, 1H), 5.47 (s, 2H). MS (m/z): $[M+H]^+$ 240.1.

3-(2,3-Dihydrobenzofuran-5-yl)-1*H*-pyrazol-5-amine (21e)

Light yellow solid. Yield: 98%. mp: 112-114 °C; ^{1}H NMR (300 MHz, DMSO-d_6) δ: 10.68 (s, 1H), 7.55 (d, J = 1.8 Hz, 1H), 7.42 (dd, J = 8.2, 1.8 Hz, 1H), 6.77 (d, J = 8.2 Hz, 1H), 5.75 (s, 1H), 4.54 (t, J = 8.7 Hz, 2H), 3.20 (t, J = 8.7 Hz, 2H). MS (m/z): $[M+H]^+$ 202.3.

3-(3,4-Dimethoxyphenyl)-1*H*-pyrazol-5-amine (21f)

Yellow solid. Yield: 93%. mp: 131-133 °C; ^{1}H NMR (300 MHz, DMSO-d_6) δ: 10.71 (s, 1H), 7.30 (d, J = 2.0 Hz, 1H), 7.20 (dd, J = 8.4, 2.0 Hz, 1H), 6.96 (d, J = 8.4 Hz, 1H), 5.80 (s, 1H), 3.80 (s, 3H), 3.77 (s, 3H). MS (m/z): $[M+H]^+$ 220.4.

General procedure for the synthesis of compound 22a-22i. To a stirring solution of methyl-5-bromopicolinate (0.5 g, 2.31 mmol) in anhydrous toluene (15 mL) were added 1-methylpiperidin-4-amine (0.26 g, 2.31 mmol), $Pd(OAc)_2$ (0.22 g, 0.1 mmol), BINAP (0.62 g, 0.1 mmol) and Cs_2CO_3 (1.37 g, 2.2 mmol) under an argon atmosphere. Reaction was stirred at 90 ℃ for 12 h. Upon completion, the reaction mixture was filtered over celite and rinsed with ethyl acetate. The mixture was extracted with ethyl acetate (40 mL × 3). Then, the combined organic phase was concentrated in vacuo and purified by silica gel column chromatography (EA : MeOH = 20 : 1) to afford compound **22a** as a white solid. Yield: 50%. mp: 138-140 °C; ^{1}H NMR (400 MHz, DMSO-d_6) δ: 8.02 (d, J = 2.8 Hz, 1H), 7.78 (d, J = 8.7 Hz, 1H), 6.93 (dd, J = 8.7, 2.8 Hz, 1H), 6.68 (d, J = 7.5 Hz, 1H), 3.76 (s, 3H), 3.32−3.25 (m, 1H), 2.72 (dd, J = 12.0, 3.9 Hz, 2H), 2.16 (s, 3H), 2.02 (td, J = 11.4, 2.7 Hz, 2H), 1.90−1.82 (m, 2H), 1.42 (qd, J = 11.2, 3.8 Hz, 2H). MS (m/z): $[M+H]^+$ 250.3.

Methyl-3-chloro-4-((1-methylpiperidin-4-yl)amino)benzoate (22b)

Brown solid was afforded as the crude product which was used in next step without further purification.

Methyl-3-methyl-4-((1-methylpiperidin-4-yl)amino)benzoate (22c)

Brown solid. Yield: 59%. mp: 110-112 °C; ^{1}H NMR (400 MHz, DMSO-d_6) δ: 7.64 (dd, J = 8.7, 2.2 Hz, 1H), 7.58−7.55 (m, 1H), 6.61 (d, J = 8.7 Hz, 1H), 5.19 (d, J = 7.9 Hz, 1H), 3.74 (s, 3H), 3.34−3.27 (m, 1H), 2.75 (dt, J = 12.0, 3.7 Hz, 2H), 2.17 (s, 3H), 2.11 (s, 3H), 1.99 (td, J = 11.7, 2.4 Hz, 2H), 1.90−1.82 (m, 2H), 1.56 (qd, J = 12.0, 3.7 Hz, 2H). MS (m/z): $[M+H]^+$ 263.2.

Methyl-3-fluoro-4-((1-methylpiperidin-4-yl)amino)benzoate (22d)

Purple solid. Yield: 76%. mp: 96-98 °C; ^{1}H NMR (400 MHz, DMSO-d_6) δ: 7.64−7.57 (m, 1H), 7.50 (dd, J = 12.8, 2.0 Hz, 1H), 6.80 (t, J = 8.7 Hz, 1H), 6.09 (dd, J = 8.3, 2.5 Hz, 1H), 3.77 (s, 3H), 3.37−3.25 (m, 1H), 2.81−2.68 (m, 2H), 2.16 (s, 3H), 1.98 (td, J = 11.8, 2.3 Hz, 2H), 1.89−1.77 (m, 2H), 1.56 (qd, J = 12.2, 3.7 Hz, 2H). MS (m/z): $[M+H]^+$ 267.6.

Methyl-4-((1-methylpiperidin-4-yl)amino)benzoate (22e)

Brown oil. Yield: 50%; ^{1}H NMR (300 MHz, DMSO-d_6) δ: 7.67 (d, J = 8.8 Hz, 2H), 6.60 (d, J = 8.8 Hz, 2H), 6.46 (d, J = 7.7 Hz, 1H), 3.73 (s, 3H), 3.35-3.31 (m, 1H), 2.90−2.86 (m, 2H), 2.29 (s, 3H), 2.25−2.22 (m, 2H), 1.93−1.89 (m, 2H), 1.51−1.47 (m, 2H). MS (m/z): $[M+H]^+$ 249.1.

***Tert*-butyl 4-(4-(methoxycarbonyl)phenyl)piperazine-1-carboxylate (22f)**

White solid. Yield: 54%. mp: 165-166°C; ^{1}H NMR (300 MHz, $CDCl_3$) δ: 7.98−7.86 (m, 2H), 6.92−6.80 (m, 2H), 3.87 (s, 3H), 3.58 (dd, J = 6.5, 4.0 Hz, 4H), 3.30 (dd, J = 6.5, 4.0 Hz, 4H), 1.44 (s, 9H). MS (m/z): $[M- (Boc)+H]^+$ 221.2.

Methyl-4-(4-methylpiperazin-1-yl)benzoate (22g)

Red solid. Yield: 58%. mp: 105-107°C; ^{1}H NMR (300 MHz, DMSO-d_6) δ: 7.84−7.73 (m, 2H), 7.02−6.93 (m, 2H), 3.77 (s, 3H), 2.42 (dd, J = 6.0, 4.2 Hz, 4H), 2.21 (s, 3H). MS (m/z): $[M+H]^+$ 235.2.

Methyl-4-(4-ethylpiperazin-1-yl)benzoate (22h)

Grey solid. Yield: 35%. mp: 95-97°C; ^{1}H NMR (300 MHz, DMSO-d_6) δ: 7.81−7.74 (m, 2H), 7.01−6.93 (m, 2H), 3.77 (s, 3H), 3.32−3.27 (m, 4H), 2.46 (d, J = 5.0 Hz, 4H), 2.36 (q, J = 7.2 Hz, 2H), 1.03 (t, J = 7.2 Hz, 3H). MS (m/z): $[M+H]^+$ 249.2.

Methyl-4-morpholinobenzoate (22i)

White solid. Yield: 73%. mp: 162-164°C; ^{1}H NMR (300 MHz, $CDCl_3$) δ: 7.99−7.89 (m, 2H), 6.92−6.83 (m, 2H), 3.94−3.80 (m, 7H), 3.29 (t, J = 4.9 Hz, 4H). MS (m/z): $[M+H]^+$ 222.2.

General procedure for the synthesis of compound 23-27 and 45-54.

3-Chloro-*N*-(3-cyano-1*H*-pyrazol-5-yl)-4-((1-methylpiperidin-4-yl)amino)benzamide (23). To a stirring solution of compound **22b** (0.65 g, 2.31 mmol) in anhydrous toluene (3 mL) were added **20** (0.40 g, 2.10 mmol) and 2 M trimethylaluminum toluene solution (4.20 mL, 8.40 mmol) under an argon atmosphere. Reaction was stirred at 90 °C for 10 h. After this period, the reaction was quenched with 95% ethanol (40 mL). The solvent was removed in vacuo, and then purified by silica gel column chromatography (EA : MeOH = 20 : 1) to afford title compound as a white solid. Yield: 33%; mp : 156-158 °C; Peak area: 95.1%; ^{1}H NMR (300 MHz, DMSO-d_6) δ: 12.92 (brs, 1H), 10.82 (brs, 1H), 8.50 (s, 1H), 7.80 (s, 1H), 7.37−7.35 (m, 1H), 6.66−6.57 (m, 3H), 6.34 (s, 1H), 2.84 (m, 2H), 2.29 (s, 3H), 2.19−2.15 (m, 2H), 1.99−1.90 (m, 2H), 1.46−1.42 (m, 2H). HRMS-ESI m/z $[M+H]^+$ calcd for $C_{21}H_{22}ClN_6OS$: 441.1264, found: 441.1258.

***N*-(3-Cyano-1*H*-pyrazol-5-yl)-3-methyl-4-((1-methylpiperidin-4-yl)amino)benzamide (24).** The preparation of compound **24** was similar with that of compound **23** to afford title compound as a white solid. Yield: 31%; mp: 162-164 °C; Peak area: 95.6%; ^{1}H NMR (300 MHz, DMSO-d_6) δ: 12.84 (brs, 1H), 10.62 (brs, 1H), 8.48 (s, 1H), 7.78 (s, 1H), 7.40−7.37 (m, 1H), 6.46 (m, 2H), 6.04 (d, 1H), 2.88 (m, 2H), 2.37 (s, 3H), 2.28 (s, 3H), 1.99−1.92 (m, 2H), 1.68−1.65 (m, 2H), 1.24−1.19 (m, 2H). HRMS-EI m/z $[M+H]^+$ calcd for $C_{22}H_{25}N_6OS$: 421.1811, found: 421.1804.

***N*-(3-Cyano-1*H*-pyrazol-5-yl)-3-fluoro-4-((1-methylpiperidin-4-yl)amino)benzamide (25).** The preparation of compound **25** was similar with that of compound **23** to afford title compound as a white solid. Yield: 35%; mp: 148-150 °C; Peak area: 96.1%; ^{1}H NMR (300 MHz, DMSO-d_6) δ: 12.93 (brs, 1H), 10.30 (brs, 1H), 8.49 (s, 1H), 7.78 (s, 1H), 7.57−7.54 (m, 1H), 6.69−6.44 (m, 4H), 2.73 (m, 2H), 2.18−1.96 (m, 5H), 1.43−1.35 (m, 2H), 1.21−1.19 (m, 2H). HRMS-EI m/z $[M+H]^+$ calcd for $C_{21}H_{22}FN_6OS$: 425.1560, found: 425.1610.

***N*-(3-(4-Cyanothiophen-2-yl)-1*H*-pyrazol-5-yl)-5-((1-methylpiperidin-4-yl)amino)picolinamide (26).** The preparation of compound **26** was similar with that of compound **23** to afford title

compound as a white solid. Yield: 38%; mp: 151-153 °C; HPLC analysis: retention time, 4.918 min; peak area, 98.4%. ^{1}H NMR (300 MHz, DMSO-d_6) δ: 12.60 (s, 1H), 10.57 (s, 1H), 8.47 (s, 1H), 8.10 (s, 1H), 7.91 (d, J = 8.1 Hz, 1H), 7.80 (s, 1H), 7.14 (d, J = 8.1 Hz, 1H), 6.99 (s, 1H), 6.74 (s, 1H), 3.64 (m, 1H), 3.37 (m, 2H), 3.07 (m, 2H), 2.73 (s, 3H), 2.12 (m, 2H), 1.79 (m, 2H). HRMS-EI m/z $[M+H]^+$ calcd for $C_{2O}H_{22}N_7OS$: 408.1607, found: 408.1607.

5-(3-(4-((1-Methylpiperidin-4-yl)amino)benzamido)-1*H*-pyrazol-5-yl)thiophene-3-carboxamide (27). To a stirring solution of hit compound **LT-180-0712** (0.10 g, 0.25 mmol) in *tert*-butanol (10 mL) was added potassium hydroxide (0.41 g, 0.75 mmol). Reaction was heated to reflux and stirred for 10 h. Then the reaction mixture was concentrated in vacuo and purified by silica gel column chromatography (EA : MeOH = 10 : 1) to afford title compound as a yellow solid. Yield: 19%; mp: 195-197 °C; HPLC analysis: retention time, 6.873 min; peak area, 96.8%. ^{1}H NMR (300 MHz, DMSO-d_6) δ: 12.92 (brs, 1H), 10.89 (brs, 1H), 8.04 (s, 1H), 7.81 (d, J = 8.5 Hz, 3H), 7.73−7.72 (m, 1H), 7.29 (s, 1H), 6.61 (d, J = 8.2 Hz, 2H), 6.24 (s, 1H), 4.10 (s, 1H), 3.29−3.20 (m, 1H), 2.75−2.71 (m, 2H), 2.17 (s, 3H), 2.02 (t, J = 10.7 Hz, 2H), 1.90−1.86 (m, 2H), 1.46−1.36 (m, 2H). HRMS-EI m/z $[M+H]^+$ calcd for $C_{21}H_{25}FN_6O_2S$: 425.1760, found: 425.1761.

***N*-(3-(Benzo[*b*]thiophen-2-yl)-1*H*-pyrazol-5-yl)-4-((1-methylpiperidin-4-yl)amino)benzamide (45).** The preparation of compound **45** was similar with that of compound **23** to afford title compound as a pale-yellow solid. Yield: 37%; mp: 110-112 °C; HPLC analysis: retention time, 11.258 min; peak area, 96.4%. ^{1}H NMR (300 MHz, DMSO-d_6) δ: 12.88 (brs, 1H), 10.62 (s, 1H), 7.97 (d, J = 7.4 Hz, 1H), 7.85 (s, 1H), 7.82 (d, J = 8.8 Hz, 2H), 7.73 (s, 1H), 7.38−7.36 (m, 2H), 6.73 (brs, 1H), 6.64 (d, J = 8.6 Hz, 2H), 6.27 (d, J = 7.4 Hz, 1H), 3.29−3.27 (m, 1H), 2.75−2.73 (m, 2H), 2.18 (s, 3H), 2.05−2.03 (m, 2H), 1.90-1.88 (m, 2H), 1.44−1.42 (m, 2H). HRMS-ESI m/z $[M+H]^+$ calcd for $C_{24}H_{26}N_5OS$: 432.1858, found: 432.1858.

***N*-(3-(Benzo[*d*][1,3]dioxol-5-yl)-1*H*-pyrazol-5-yl)-4-((1-methylpiperidin-4-yl)amino)benzamide (46).** The preparation of compound **46** was similar with that of compound **23** to afford title compound as a white solid. Yield: 41%; mp: 286-288 °C; HPLC analysis: retention time, 7.062 min; peak area, 99.5%. ^{1}H NMR (300 MHz, DMSO-d_6) δ: 12.68 (s, 1H), 10.30 (s, 1H), 7.81 (d, J = 8.4 Hz, 2H), 7.31 (s, 1H), 7.25 (d, J = 8.0 Hz, 1H), 7.00 (d, J = 8.0 Hz, 1H), 6.91 (s, 1H), 6.60 (d, J = 8.4 Hz, 2H), 6.19 (s, 1H), 6.06 (s, 2H), 3.27−3.25 (m, 1H), 2.75 (d, J = 11.6 Hz, 2H), 2.18 (s, 3H), 2.06−2.04 (m, 2H), 1.88 (d, J = 11.6 Hz, 2H), 1.43−1.40 (m, 2H). HRMS-ESI m/z $[M+H]^+$ calcd for $C_{23}H_{26}N_5O_3$: 420.2036, found: 420.2026.

***N*-(3-(2,3-Dihydrobenzo[*b*][1,4]dioxin-6-yl)-1*H*-pyrazol-5-yl)-4-((1-methylpiperidin-4-yl)amino)benzamide (47).** The preparation of compound **47** was similar with that of compound **23** to afford title compound as a yellow solid. Yield: 47%; mp: >250°C; HPLC analysis: retention time, 10.037 min; peak area, 90.4%. ^{1}H NMR (300 MHz, DMSO-d_6) δ: 12.59 (brs, 1H), 10.28 (brs, 1H),

7.81 (d, *J* = 8.4 Hz, 2H), 7.27−7.12 (m, 2H), 6.91 (d, *J* = 8.3 Hz, 1H), 6.78 (s, 1H), 6.60 (d, *J* = 8.5 Hz, 2H), 4.29−4.28 (m, 4H), 2.76−2.72 (m, 2H), 2.18 (s, 3H), 2.08−1.98 (m, 2H), 1.90−1.86 (m, 2H), 1.48−1.36 (m, 2H). HRMS-ESI m/z $[M+H]^+$ calcd for $C_{24}H_{28}N_5O_3$: 434.2192, found: 434.2185.

***N*-(3-(2,2-Difluorobenzo[*d*][1,3]dioxol-5-yl)-1*H*-pyrazol-5-yl)-4-((1-methylpiperidin-4-yl)amino)benzamide (48).** The preparation of compound **48** was similar with that of compound **23** to afford title compound as a white solid. Yield: 41%; mp: 226-228 °C; HPLC analysis: retention time, 11.570 min; peak area, 96.7%. ^{1}H NMR (300 MHz, DMSO-d_6) δ: 12.81 (brs, 1H), 10.30 (brs, 1H), 7.80 (d, *J* = 9.3 Hz, 3H), 7.61 (d, *J* = 7.6 Hz, 1H), 7.47 (d, *J* = 6.5 Hz, 1H), 7.02 (brs, 1H), 6.62 (d, *J* = 7.2 Hz, 2H), 6.13 (s, 1H), 2.78−2.76 (m, 2H), 2.20 (s, 3H), 2.10−2.08 (m, 2H), 1.90−1.88 (m, 2H), 1.48−1.45 (m, 2H). HRMS-ESI m/z $[M+H]^+$ calcd for $C_{23}H_{24}N_5O_3F_2$: 456.1847, found: 456.1849.

***N*-(3-(2,3-Dihydrobenzofuran-5-yl)-1*H*-pyrazol-5-yl)-4-((1-methylpiperidin-4-yl)amino)benzamide (49).** The preparation of compound **49** was similar with that of compound **23** to afford title compound as a pale-yellow solid. Yield: 12%; mp: 202-204 °C; HPLC analysis: retention time, 9.890 min; peak area, 95.4%. ^{1}H NMR (300 MHz, DMSO-d_6) δ: 10.44 (s, 1H), 7.80 (d, *J* = 8.7 Hz, 3H), 7.62 (s, 1H), 7.47 (d, *J* = 8.3 Hz, 1H), 6.83 (s, 1H), 6.78 (d, *J* = 7.2 Hz, 1H), 6.58 (d, *J* = 8.8 Hz, 2H), 6.19 (d, *J* = 7.7 Hz, 1H), 4.56 (t, 2H), 3.29−3.28 (m, 1H), 3.22 (t, 2H), 2.74−2.72 (m, 2H), 2.18 (s, 3H), 2.06−2.02 (m, 2H), 1.92−1.89 (m, 2H), 1.43−1.39 (m, 2H). HRMS-ESI m/z $[M+H]^+$ calcd for $C_{24}H_{28}N_5O_2$: 418.2243, found: 418.2234.

***N*-(3-(3,4-Dimethoxyphenyl)-1*H*-pyrazol-5-yl)-4-((1-methylpiperidin-4-yl)amino)benzamide (50).** The preparation of compound **50** was similar with that of compound **23** to afford title compound as a pale-yellow solid. Yield: 21%; mp: >250°C; HPLC analysis: retention time, 5.719 min; peak area, 97.0%. ^{1}H NMR (300 MHz, DMSO-d_6) δ: 10.79 (brs, 1H), 7.85 (d, *J* = 8.6 Hz, 2H), 7.38 (s, 1H), 7.28 (d, *J* = 6.6 Hz, 1H), 7.01 (d, *J* = 8.4 Hz, 1H), 6.85 (s, 1H), 6.60 (d, *J* = 8.7 Hz, 2H), 6.22 (d, *J* = 7.7 Hz, 1H), 3.84 (s, 3H), 3.78 (s, 3H), 3.28−3.26 (m, 1H), 2.75−2.73 (m, 2H), 2.17 (s, 3H), 2.04−2.01 (m, 2H), 1.90−1.88 (m, 2H), 1.43−1.39 (m, 2H). ^{13}C NMR (75 MHz, DMSO-d_6) δ: 164.54 (s), 151.27 (s), 149.33 (s), 148.90 (s), 129.88 (s), 120.37 (s), 117.85 (s), 112.45 (s), 111.51 (s), 109.06 (s), 55.99 (s), 54.58 (s), 48.77 (s), 46.48 (s), 32.02 (s), 25.16 (s). HRMS-ESI m/z $[M+H]^+$ calcd for $C_{24}H_{30}N_5O_3$: 436.2349, found: 436.2344.

***N*-(3-(benzo[*d*][1,3]dioxol-5-yl)-1*H*-pyrazol-5-yl)-4-(piperazin-1-yl)benzamide (51).** The preparation of compound **51** was similar with that of compound **23** to afford title compound as orange solid. Yield: 16%; mp: >300 °C; HPLC analysis: retention time, 5.779 min; peak area, 95.0%. ^{1}H NMR (600 MHz, DMSO-d_6) δ: 10.74 (s, 1H), 9.48 (s, 2H), 8.00−7.98 (d, *J* = 8.8 Hz, 2H), 7.36 (s, 1H), 7.29−7.28 (d, *J* = 8.1, 1.7 Hz, 1H), 7.07−7.06 (d, *J* = 8.9 Hz, 2H), 7.01−7.00 (d,

J = 8.1 Hz, 1H), 6.86 (s, 1H), 6.07 (s, 2H), 3.57−3.55 (m, 4H), 3.22−3.17 (m, 4H). ^{13}C NMR (126 MHz, DMSO-d_6) δ: 164.48 (s), 152.64 (s), 148.29 (s), 147.77 (s), 146.70 (s), 143.97 (s), 129.82 (s), 124.49 (s), 124.10 (s), 119.74 (s), 114.64 (s), 109.21 (s), 106.14 (s), 101.77 (s), 94.14 (s), 45.82 (s), 44.66 (s), 42.71 (s), 8.89 (s), 8.13 (s). HRMS-ESI m/z $[M+H]^+$ calcd for $C_{21}H_{22}N_5O_3$: 392.1723, found: 392.1718.

***N*-(3-(benzo[*d*][1,3]dioxol-5-yl)-1*H*-pyrazol-5-yl)-4-(4-methylpiperazin-1-yl)benzamide (52).** The preparation of compound **52** was similar with that of compound **23** to afford title compound as white solid. Yield: 20%; mp: 263-265 °C; HPLC analysis: retention time, 3.346 min; peak area, 99.6%. ^{1}H NMR (600 MHz, DMSO-d_6) δ: 12.71 (s, 1H), 10.47 (s, 1H), 7.93 (d, *J* = 8.6 Hz, 2H), 7.32 (s, 1H), 7.25 (d, *J* = 8.0 Hz, 1H), 7.01 (d, *J* = 8.1 Hz, 1H), 6.98 (d, *J* = 8.7 Hz, 2H), 6.93 (s, 1H), 6.08 (s, 2H), 3.29−3.28 (m, 4H), 2.46−2.45 (m, 4H), 2.23 (s, 3H). ^{13}C NMR (126 MHz, DMSO-d_6) δ: 164.58 (s), 153.44 (s), 149.06 (s), 148.32 (s), 147.56 (s), 142.07 (s), 129.61 (s), 124.17 (s), 123.47 (s), 119.33 (s), 113.89 (s), 109.26 (s), 105.90 (s), 101.73 (s), 94.92 (s), 54.87 (s), 47.36 (s), 46.21 (s). HRMS-ESI m/z $[M+H]^+$ calcd for $C_{22}H_{24}N_5O_3$: 406.1879, found: 406.1880.

***N*-(3-(benzo[*d*][1,3]dioxol-5-yl)-1*H*-pyrazol-5-yl)-4-(4-ethylpiperazin-1-yl)benzamide (53).** The preparation of compound **53** was similar with that of compound **23** to afford title compound as white solid. Yield: 31%; mp: 240-242 °C; HPLC analysis: retention time, 3.567 min; peak area, 98.6%. ^{1}H NMR (600 MHz, DMSO-d_6) δ: 12.71 (s, 1H), 10.48 (s, 1H), 7.94 (d, *J* = 8.5 Hz, 2H), 7.32 (s, 1H), 7.26−7.25 (t, 1H), 7.02−6.98 (m, 3H), 6.93 (s, 1H), 6.08 (s, 2H), 3.30−3.28 (m, 4H), 2.49−2.48 (m, 4H), 2.38 (q, *J* = 6 Hz, 2H), 1.05 (t, *J* = 6 Hz, 3H). ^{13}C NMR (126 MHz, DMSO-d_6) δ: 164.58 (s), 153.48 (s), 149.08 (s), 148.31 (s), 147.55 (s), 142.06 (s), 129.61 (s), 124.19 (s), 123.45 (s), 119.32 (s), 113.84 (s), 109.25 (s), 105.90 (s), 101.72 (s), 94.91 (s), 55.38 (s), 52.63 (s), 52.09 (s), 47.48 (s), 12.44 (s). HRMS-ESI m/z $[M+H]^+$ calcd for $C_{23}H_{26}N_5O_3$: 420.2036, found: 420.2035.

***N*-(3-(benzo[*d*][1,3]dioxol-5-yl)-1*H*-pyrazol-5-yl)-4-morpholinobenzamide (54).** The preparation of compound **54** was similar with that of compound **23** to afford title compound as white solid. Yield: 17%; mp: 264-266 °C; HPLC analysis: retention time, 2.800 min; peak area, 97.6%. ^{1}H NMR (600 MHz, DMSO-d_6) δ: 12.72 (s, 1H), 10.51 (s, 1H), 7.97−7.95 (d, *J* = 8.4 Hz, 2H), 7.33 (s, 1H), 7.26−7.25 (d, *J* = 8.1 Hz, 1H), 7.02 (s, 1H), 6.99 (d, *J* = 9.2 Hz, 2H), 6.95 (s, 1H), 6.08 (s, 2H), 3.76−3.74 (m, 4H), 3.34−3.24 (m, 4H). ^{13}C NMR (126 MHz, DMSO-d_6) δ: 164.56 (s), 153.59 (s), 149.04 (s), 148.33 (s), 147.57 (s), 142.08 (s), 129.59 (s), 124.17 (s), 124.00 (s), 119.34 (s), 113.78 (s), 109.27 (s), 105.90 (s), 101.74 (s), 94.93 (s), 66.42 (s), 47.73 (s), 30.79 (s). HRMS-ESI m/z $[M+H]^+$ calcd for $C_{21}H_{21}N_4O_4$: 393.1563, found: 393.1557.

General procedure for the synthesis of compound 35a-35g. To a stirring solution of

2-bromothiophene (2.0 g, 12.3 mmol) in acetic anhydride (2.51 g, 24.6 mmol) was added perchloric acid (3.71 g, 36.9 mmol) dropwise in ice bath for 0.5 h. Then, reaction was stirred at r.t. for 6 h. Upon completion, the reaction mixture was taken up in ice water (60 mL), the pH was adjusted to 6-7 with sodium carbonate, and the aqueous phase was extracted with ethyl acetate (25 mL × 3). The combined organic phase was washed twice with saturated brine (20 mL × 2) and dried over anhydrous $MgSO_4$. After filtering out $MgSO_4$, the filtrate was concentrated in vacuo, followed by further purification by silica gel column chromatography (PE : EA=50 : 1) to afford compound **35b** as a yellow solid; Yield: 70%. mp: 93-95 °C; ^{1}H NMR (300 MHz, $CDCl_3$) δ: 7.42 (d, J = 4.0 Hz, 1H), 7.10 (d, J = 4.0 Hz, 1H), 2.52 (s, 3H). MS (m/z): $[M+H]^+$ 204.9, 206.9.

1-(4-Bromothiophen-2-yl)ethan-1-one (35a)

Light yellow oil was afforded as the crude product which was used in next step without further purification. MS (m/z): $[M+H]^+$ 204.9, 206.9.

1-(4-Methoxythiophen-2-yl)ethan-1-one (35c)

Colorless oil. Yield: 45%; ^{1}H NMR (300 MHz, $CDCl_3$) δ: 7.42 (d, J = 4.0 Hz, 1H), 7.10 (d, J = 4.0 Hz, 1H), 3.99 (s, 3H), 2.53 (s, 3H). MS (m/z): $[M+H]^+$ 157.0.

1-(5-Methoxythiophen-2-yl)ethan-1-one (35d)

Light yellow oil. Yield: 53%; ^{1}H NMR (300 MHz, DMSO-d_6) δ: 7.92 (d, J = 5.5 Hz, 1H), 7.16 (d, J = 5.5 Hz, 1H), 3.98 (s, 3H), 2.43 (s, 3H). MS (m/z): $[M+H]^+$ 157.1.

1-(5-Chlorothiophen-2-yl)ethan-1-one (35e)

Brown solid. Yield: 81%. mp: 46-48 °C; ^{1}H NMR (300 MHz, DMSO-d_6) δ: 7.86 (d, J = 4.1 Hz, 1H), 7.30 (d, J = 4.1 Hz, 1H), 2.51 (s, 3H). MS (m/z): $[M+H]^+$ 161.0, 163.0.

1-(4-Chlorothiophen-2-yl)ethan-1-one (35f)

White solid. Yield: 81%. mp: 49-51 °C; ^{1}H NMR (300 MHz, DMSO-d_6) δ: 7.86 (s, 1H), 7.30 (s, 1H), 2.51 (s, 3H). MS (m/z): $[M+H]^+$ 161.0, 163.0.

1-(Thiophen-2-yl)ethan-1-one (35g)

Brown oil. Yield: 60%; ^{1}H NMR (300 MHz, DMSO-d_6) δ: 8.00 (d, J = 4.9 Hz, 1H), 7.94 (d, J = 3.6 Hz, 1H), 7.26 (t, J = 4.2 Hz, 1H), 2.56 (s, 3H). MS (m/z): $[M+H]^+$ 127.1.

General procedure for the synthesis of compound 35h-35k. To a stirring solution of 2-bromothiophene (3.44 g, 21.1 mmol) in CH_3CN (10 mL) were added 3-cyclopentylpropionic acid (1.00 g, 7.03 mmol) and phosphoric acid (0.81 g, 7.03 mmol). Reaction was stirred at r.t. for 3 h. Then, the pH of reaction mixture was adjusted to 6-7 with sodium carbonate, and the aqueous phase was extracted with ethyl acetate (25 mL × 3). The combined organic phase was washed twice with saturated brine (20 mL × 2) and dried over anhydrous $MgSO_4$. After filtering out $MgSO_4$, the filtrate was concentrated in vacuo, followed by further purification by silica gel column chromatography (PE : EA = 50 : 1) chromatography to afford compound **35h** as a white

solid; Yield: 54%; mp: 34-36 °C; ^{1}H NMR (300 MHz, $CDCl_3$) δ: 7.45 (d, J= 4.0 Hz, 1H), 7.10 (d, J= 4.0 Hz, 1H), 2.88−2.77 (m, 2H), 1.85−1.67 (m, 5H), 1.67−1.57 (m, 2H), 1.54−1.51 (m, 2H), 1.14−1.05 (m, 2H). MS (m/z): $[M+H]^+$ 287.0

1-(5-Bromothiophen-2-yl)-2-cyclopentylethan-1-one (35h)

White solid. Yield: 55%. mp: 34-36 °C; ^{1}H NMR (300 MHz, $CDCl_3$) δ: 7.45 (d, J = 4.0 Hz, 1H), 7.10 (d, J = 4.0 Hz, 1H), 2.88−2.77 (m, 2H), 1.85−1.67 (m, 5H), 1.67−1.57 (m, 2H), 1.54−1.51 (m, 2H), 1.14−1.05 (m, 2H). MS (m/z): $[M+H]^+$ 273.0, 275.0

1-(5-Bromothiophen-2-yl)-2-phenylethan-1-one (35i)

White solid. Yield: 86%. mp: 52-53 °C; ^{1}H NMR (300 MHz, $CDCl_3$) δ: 7.40 (d, J = 4.0 Hz, 1H), 7.32−7.28 (m, 1H), 7.26−7.17 (m, 4H), 7.07 (d, J = 4.0 Hz, 1H), 3.18−3.12 (m, 2H), 3.06−3.01 (m, 2H). MS (m/z): $[M+H]^+$ 281.0, 283.0

1-(5-Chlorothiophen-2-yl)-2-(4-(trifluoromethyl)phenyl)ethan-1-one (35j)

White solid. Yield: 75%. mp: 47-48 °C; ^{1}H NMR (300 MHz, DMSO-d_6) δ: 7.93 (d, J = 4.1 Hz, 1H), 7.64 (d, J = 8.1 Hz, 2H), 7.51 (d, J = 8.0 Hz, 2H), 7.30 (d, J = 4.1 Hz, 1H), 3.35 (t, J = 9.2 Hz, 2H), 3.01 (t, J = 7.5 Hz, 2H). MS (m/z): $[M+H]^+$ 305.0, 307.0

1-(5-Chlorothiophen-2-yl)-2-(4-methoxyphenyl)ethan-1-one (35k)

White solid. Yield: 80%. mp: 41-42 °C; ^{1}H NMR (300 MHz, DMSO-d_6) δ: 7.89 (d, J = 4.1 Hz, 1H), 7.28 (d, J = 4.1 Hz, 1H), 7.17 (d, J = 8.5 Hz, 2H), 6.83 (d, J = 8.6 Hz, 2H), 3.71 (s, 3H), 3.22 (t, J = 7.5 Hz, 2H), 2.85 (t, J = 7.5 Hz, 2H). MS (m/z): $[M+Na]^+$ 303.0, 305.0.

General procedure for the synthesis of compound 36a-36b. In a sealed tube, compound **35a** (2.0 g, 9.75 mmol) was dissolved in anhydrous DMF (6 mL), followed by the addition of cuprous cyanide (2.62 g, 29.26 mmol) and potassium iodide (0.017 g, 0.1 mmol) under an argon atmosphere. Reaction was heated to reflux and stirred for 12 h. Upon completion, the reaction was quenched with a mixture of ammonia water and ice water (v / v = 1 : 3, 40 mL). The residue was filtered and rinsed with ethyl acetate. The aqueous phase of filtrate was extracted with ethyl acetate (25 mL × 3). The combined organic phase was washed twice with saturated brine (20 mL × 2) and dried over anhydrous $MgSO_4$. After filtering out $MgSO_4$, the filtrate was concentrated in vacuo, followed by further purification by silica gel column chromatography (PE : EA = 50 : 1) to afford compound **36a** as a yellow oil. Yield: 64%. ^{1}H NMR (300 MHz, DMSO-d_6) δ: 8.08 (d, J = 4.0 Hz, 1H), 8.05 (d, J = 4.0 Hz, 1H), 2.62 (s, 3H). MS (m/z): $[M+H]^+$ 152.0.

5-acetylthiophene-2-carbonitrile (36b)

Light yellow oil. Yield: 64%; ^{1}H NMR (300 MHz, $CDCl_3$) δ: 7.67 (d, J = 5.1 Hz, 1H), 7.40 (d, J = 5.1Hz, 1H), 2.77 (s, 3H). MS(m/z): $[M+H]^+$ 152.0.

General procedure for the synthesis of compound 37a-37m. A mixture of 60% NaH (0.16 g, 3.95 mmol) and anhydrous THF and DMF (v / v = 1 : 1, 20 mL) was added compound **35f** (0.54 g,

2.63 mmol) in ice bath, and stirred for 0.5 h. Solution of compound **6a** in anhydrous THF and DMF solution (5 mL) was added dropwise for 0.5 h. Reaction was stirred at r.t. for 6 h. Upon completion, the reaction was quenched with ice water (50 mL). The pH was adjusted to 3-4 with 2N aqueous hydrochloric acid. After this period, the orange precipitates were filtered to afford the crude product **37f** which was used in next step without further purification. MS (m/z): $[M+H]^+$ 394.1.

General procedure for the synthesis of compound 28-34 and 38-44.

5-(5-((4-(4-Methylpiperazin-1-yl)phenyl)amino)-1*H*-pyrazol-3-yl)thiophene-3-carbonitrile (28). To a stirring solution of compound **37l** (0.30 g, 0.78 mmol) in anhydrous ethanol (10 mL) was added 85% hydrazine hydrate (0.047 g, 0.94 mmol). Reaction was heated to reflux and stirred for 6 h. Then, the mixture was concentrated in vacuo, and the residue was purified by silica gel column chromatography (DCM : MeOH = 20 : 1) to afford title compound as a white solid. Yield: 20%; mp: 206-208 °C; HPLC analysis: retention time, 2.823 min; peak area, 98.8%. ^{1}H NMR (300 MHz, DMSO-d_6) δ: 12.40 (s, 1H), 8.17 (s, 1H), 7.61 (s, 1H), 7.34−6.90 (m, 3H), 6.86 (d, J = 8.5 Hz, 2H), 6.34 (s, 1H), 2.99 (t, J = 4.3 Hz, 4H), 2.43 (t, J = 4.3 Hz, 4H), 2.20 (s, 3H). ^{13}C NMR (151 MHz, DMSO-d_6) δ: 170.80 (s), 144.74 (s), 136.89 (s), 131.69 (s), 126.24 (s), 117.51 (s), 116.79 (s), 60.24 (s), 55.27 (s), 49.86 (s), 46.25 (s), 21.24 (s), 14.57 (s). HRMS-EI m/z $[M+H]^+$ calcd for $C_{26}H_{29}ClN_5OS$: 365.1548, found: 365.1522.

3-(4-Bromothiophen-2-yl)-*N*-(4-(4-methylpiperazin-1-yl)phenyl)-1*H*-pyrazol-5-amine (29). The preparation of compound **29** was similar with that of compound **28** to afford title compound as a white solid. Yield: 17%. mp: 178-180 °C; HPLC analysis: retention time, 15.844 min; peak area, 97.4%. ^{1}H NMR (300 MHz, DMSO-d_6) δ: 12.40 (brs, 1H), 8.13 (d, J = 13.9 Hz, 1H), 7.15 (m, 3H), 6.85 (d, J = 8.3 Hz, 2H), 6.37−6.04 (m, 1H), 3.00 (t, J = 4.6 Hz, 4H), 2.42 (t, J = 4.6 Hz, 4H), 2.21 (s, 3H). ^{13}C NMR (151 MHz, DMSO-d_6) δ: 144.91 (s), 136.91 (s), 131.69 (s), 126.18 (s), 117.51 (s), 116.80 (s), 109.60 (s), 55.26 (s), 49.91 (s), 49.86 (s), 46.24 (s); HRMS-EI m/z $[M+H]^+$ calcd for $C_{18}H_{21}BrN_5S$: 418.0701, found: 418.0701.

3-(4-Chlorothiophen-2-yl)-*N*-(4-(4-methylpiperazin-1-yl)phenyl)-1*H*-pyrazol-5-amine (30). The preparation of compound **30** was similar with that of compound **28** to afford title compound as a white solid. Yield: 17%; mp: 178-180 °C; HPLC analysis: retention time, 15.276 min; peak area, 96.0%. ^{1}H NMR (300 MHz, Acetone-d_6) δ: 7.38 (d, J = 5.4 Hz, 1H), 7.31 (s, 1H), 7.05 (d, J = 8.7 Hz, 2H), 6.92 (d, J = 5.4 Hz, 1H), 6.77 (d, J = 8.9 Hz, 2H), 6.25 (s, 1H), 2.96−2.90 (m, 4H), 2.39−2.33 (m, 4H), 2.12 (s, 3H). HRMS-EI m/z $[M+H]^+$ calcd for $C_{18}H_{21}ClN_5S$: 374.1206, found: 374.1190.

3-(4-Methoxythiophen-2-yl)-*N*-(4-(4-methylpiperazin-1-yl)phenyl)-1*H*-pyrazol-5-amine (31). The preparation of compound **31** was similar with that of compound **28** to afford title compound

as a white solid. Yield: 32%; mp: 233-235 °C; HPLC analysis: retention time, 10.984 min; peak area, 96.4%. ^{1}H NMR (300 MHz, DMSO-d_6) δ: 11.91 (s, 1H), 8.05 (s, 1H), 7.43 (s, 1H), 7.35−7.07 (m, 3H), 6.82 (d, J = 8.5 Hz, 2H), 5.98 (s, 1H), 3.88 (s, 3H), 3.00−2.97 (m, 4H), 2.45−2.42 (m, 4H), 2.21 (s, 3H). ^{13}C NMR (151 MHz, DMSO-d_6) δ: 154.47 (s), 144.18 (s), 137.42 (s), 123.89 (s), 117.75 (s), 117.49 (s), 116.46 (s), 90.89 (s), 67.48 (s), 59.11 (s), 55.29 (s), 50.01 (s), 46.24 (s), 25.60 (s); HRMS-EI m/z $[M+H]^+$ calcd for $C_{19}H_{24}N_5OS$: 370.1702, found: 370.1677.

3-(5-Bromothiophen-2-yl)-*N*-(4-(4-methylpiperazin-1-yl)phenyl)-1*H*-pyrazol-5-amine (32). The preparation of compound **32** was similar with that of compound **28** to afford title compound as a pale-yellow solid. Yield: 38%; mp: 142-145 °C; ^{1}H NMR (300 MHz, DMSO-d_6) δ: 12.38−12.15 (m, 1H), 8.10−8.03 (m, 1H), 7.22−6.82 (m, 6H), 6.12−6.00 (m, 1H), 3.31−2.43 (m, 8H), 2.21 (s, 3H). HRMS-ESI m/z $[M+H]^+$ calcd for $C_{18}H_{21}BrN_5S$: 418.0701, found: 418.0689.

3-(5-Chlorothiophen-2-yl)-*N*-(4-(4-methylpiperazin-1-yl)phenyl)-1*H*-pyrazol-5-amine (33). The preparation of compound **33** was similar with that of compound **28** to afford title compound as a white solid. Yield: 21%; mp: 200-204 °C; HPLC analysis: retention time, 3.674 min; peak area, 98.3%. ^{1}H NMR (300 MHz, DMSO-d_6) δ: 12.37−12.19 (m, 1H), 8.08 (s, 1H), 7.23−6.82 (m, 6H), 6.07 (s, 1H), 2.99 (t, J = 4.7 Hz, 4H), 2.44 (t, J = 4.7 Hz, 4H), 2.21 (s, 3H). ^{13}C NMR (151 MHz, DMSO-d_6) δ: 153.54 (s), 145.51 (s), 144.58 (s), 136.88 (s), 131.50 (s), 127.95 (s), 123.42 (s), 117.51 (s), 116.83 (s), 91.08 (s), 88.22 (s), 67.49 (s), 55.26 (s), 49.90 (s), 46.25 (s), 25.61 (s). HRMS-EI m/z $[M+H]^+$ calcd for $C_{18}H_{21}ClN_5S$: 374.1206, found: 374.1192.

3-(5-Methoxythiophen-2-yl)-*N*-(4-(4-methylpiperazin-1-yl)phenyl)-1*H*-pyrazol-5-amine (34). The preparation of compound **34** was similar with that of compound **28** to afford title compound as a white solid. Yield: 25%; mp: 200-202 °C; HPLC analysis: retention time, 3.129 min; peak area, 98.6%. ^{1}H NMR (300 MHz, DMSO-d_6) δ: 12.17−11.96 (m, 1H), 8.05 (s, 1H), 7.40−6.89 (m, 3H), 6.84 (d, J = 8.4 Hz, 2H), 6.30 (s, 1H), 5.87 (s, 1H), 3.87 (s, 3H), 2.99 (t, J = 4.6 Hz, 4H), 2.44 (t, J = 4.6 Hz, 4H), 2.21 (s, 3H). ^{13}C NMR (151 MHz, DMSO-d_6) δ: 165.23 (s), 153.13 (s), 144.37 (s), 137.22 (s), 122.36 (s), 117.50 (s), 116.60 (s), 104.89 (s), 90.03 (s), 60.67 (s), 55.38 (s), 49.98 (s), 46.24 (s). HRMS-EI m/z $[M+H]^+$ calcd for $C_{19}H_{24}N_5OS$: 370.1702, found: 370.1675.

5-(5-((4-(4-Methylpiperazin-1-yl)phenyl)amino)-1*H*-pyrazol-3-yl)thiophene-2-carbonitrile (38). The preparation of compound **38** was similar with that of compound **28** to afford title compound as a white solid. Yield: 28%; mp: 202-204 °C; HPLC analysis: retention time, 7.889 min; peak area, 99.7%. ^{1}H NMR (300 MHz, DMSO-d_6) δ: 12.54 (s, 1H), 8.18 (s, 1H), 7.92 (d, J = 3.6 Hz, 1H), 7.52 (d, J = 3.8 Hz, 1H), 7.05−7.02 (m, 2H), 6.85 (d, J = 8.5 Hz, 2H), 6.28 (s, 1H), 3.00 (t, J = 4.8 Hz, 4H), 2.45 (t, J = 4.8 Hz, 4H), 2.21 (s, 3H). ^{13}C NMR (151 MHz, DMSO-d_6) δ: 145.41 (s), 140.21 (s), 136.53 (s), 124.60 (s), 117.53 (s), 117.10 (s), 115.11 (s), 105.95 (s), 89.95

(s), 55.24 (s), 49.81 (s), 46.24 (s). HRMS-EI m/z $[M+H]^+$ calcd for $C_{19}H_{21}N_6S$: 365.1548, found: 365.1522.

5-(5-((4-(4-Methylpiperazin-1-yl)phenyl)amino)-1*H*-pyrazol-3-yl)thiophene-2-carboxamide (39). The preparation of compound **39** was similar with that of compound **28** to afford title compound as a pale-green solid. Yield: 34%; mp: 208-212 °C; HPLC analysis: retention time, 7.097 min; peak area, 95.5%. ^{1}H NMR (300 MHz, DMSO-d_6) δ: 12.26 (s, 1H), 7.99 (s, 1H), 7.69 (d, J = 3.8 Hz, 1H), 7.41 (s, 1H), 7.36 (d, J = 3.8 Hz, 1H), 7.11 (s, 2H), 6.85 (d, J = 8.9 Hz, 2H), 6.10 (s, 1H), 3.01 (t, J = 4.3 Hz, 4H), 2.27 (t, J = 4.3 Hz, 4H), 1.91 (s, 3H). HRMS-EI m/z $[M+H]^+$ calcd for $C_{19}H_{23}N_6OS$: 383.1654, found: 383.1631.

***N*-(4-(4-Methylpiperazin-1-yl)phenyl)-3-(thiophen-2-yl)-1*H*-pyrazol-5-amine (40).** The preparation of compound **40** was similar with that of compound **28** to afford title compound as a white solid. Yield: 18%; mp: 212-214 °C; HPLC analysis: retention time, 13.145 min; peak area, 99.2%. ^{1}H NMR (300 MHz, DMSO-d_6) δ: 12.33−12.12 (m, 1H), 7.51 (s, 1H), 7.38 (s, 1H), 7.22 (s, 1H), 7.10 (s, 2H), 6.83 (d, J = 8.8 Hz, 2H), 5.99 (s, 1H), 2.98 (t, J = 4.6 Hz, 4H), 2.46 (t, J = 4.6 Hz, 4H), 2.22 (s, 3H). HRMS-EI m/z $[M+H]^+$ calcd for $C_{18}H_{22}N_5S$: 340.1596, found: 340.1570.

3-(5-Bromothiophen-2-yl)-4-(cyclopentylmethyl)-*N*-(4-(4-methylpiperazin-1-yl)phenyl)-1*H*-pyrazol-5-amine (41). The preparation of compound **41** was similar with that of compound **28** to afford title compound as a white solid. Yield: 53%; mp: 180-182 °C; HPLC analysis: retention time, 10.623 min; peak area, 95.2%. ^{1}H NMR (300 MHz, DMSO-d_6) δ: 12.63−12.28 (m, 1H), 7.60−6.97 (m, 4H), 6.80 (d, J = 8.5 Hz, 1H), 6.63 (s, 1H), 3.01−2.93 (m, 4H), 2.48−2.39 (m, 4H), 2.21 (s, 3H), 2.03−1.93 (m, 1H), 1.65−1.00 (m, 8H). HRMS-ESI m/z $[M+H]^+$ calcd for $C_{24}H_{31}BrN_5S$: 500.1484, found: 500.1467.

4-Benzyl-3-(5-bromothiophen-2-yl)-*N*-(4-(4-methylpiperazin-1-yl)phenyl)-1*H*-pyrazol-5-amine (42). The preparation of compound **42** was similar with that of compound **28** to afford title compound as a white solid. Yield: 49%; mp: 228-230 °C; HPLC analysis: retention time, 16.810 min; peak area, 97.3%. ^{1}H NMR (300 MHz, DMSO-d_6) δ: 12.51 (brs, 1H), 10.06 (s, 1H), 7.72 (s, 1H), 7.28−7.06 (m, 7H), 6.88−6.85 (m, 3H), 3.96 (s, 2H), 2.85 (s, 4H). HRMS-ESI m/z $[M+H]^+$ calcd for $C_{25}H_{27}BrN_5S$: 508.1171, found: 508.1161.

3-(5-Chlorothiophen-2-yl)-*N*-(4-(4-methylpiperazin-1-yl)phenyl)-4-(4-(trifluoromethyl)benzyl)-1*H*-pyrazol-5-amine (43). The preparation of compound **43** was similar with that of compound **28** to afford title compound as a white solid. Yield: 40%; mp: 224-226 °C; HPLC analysis: retention time, 7.642 min; peak area, 97.2%. ^{1}H NMR (300 MHz, DMSO-d_6) δ: 7.64−7.58 (m, 3H), 7.31 (d, J = 8.5 Hz, 2H), 7.17−6.86 (m, 4H), 6.80 (d, J = 8.9 Hz, 2H), 4.05 (s, 2H), 2.96 (t, J = 4.8 Hz, 4H), 2.43 (t, J = 4.0 Hz, 4H), 2.20 (s, 3H). ^{13}C NMR (151 MHz, DMSO-d_6) δ: 145.85

(s), 144.66 (s), 138.06 (s), 128.99 (s), 127.87 (s), 127.17 (s), 125.76 (s), 125.56 (s), 123.96 (s), 117.48 (s), 116.35 (s), 55.23 (s), 49.96 (s), 46.18 (s), 27.97 (s). HRMS-EI m/z $[M+H]^+$ calcd for $C_{26}H_{26}ClF_3N_5S$: 532.1550, found: 532.1523.

3-(5-Chlorothiophen-2-yl)-4-(4-methoxybenzyl)-*N*-(4-(4-methylpiperazin-1-yl)phenyl)-1*H*-pyrazol-5-amine (44). The preparation of compound **44** was similar with that of compound **28** to afford title compound as a white solid. Yield: 38%; mp: 228-230 °C; HPLC analysis: retention time, 12.547 min; peak area, 95.9%. ^{1}H NMR (300 MHz, DMSO-d_6) δ: 10.21 (s, 1H), 7.62 (d, J = 3.7 Hz, 2H), 7.59 (s, 1H), 7.31 (d, J = 8.1 Hz, 2H), 7.07 (s, 2H), 6.97 (s, 1H), 6.79 (d, J = 8.8 Hz, 2H), 4.04 (s, 2H), 3.01−2.91 (m, 4H), 2.47−2.38 (m, 4H), 2.20 (s, 3H). HRMS-EI m/z $[M+H]^+$ calcd for $C_{26}H_{29}ClN_5OS$: 494.1781, found: 494.1753.

Kinase Inhibition Assay. Activity of kinases were determined using Hot-Spot^{SM} kinase assay which was performed by Reaction Biology Corp. (Malvern PA, USA) as described previously.[23]

Cell Growth Inhibition Assay. The human cancer cell lines were purchased from the American Type Culture Collection (ATCC, Manassas, VA, USA). The cell lines (MV4-11, MCF-7, HT-29, Hep G2, ACHN, A-549, SK-OV-3, BxPC-3, PC-3, MKN-45, U251, KYSE-520, K-562, HL-60, Molm-13, RPMI 8226, OCI-LY19, parental BaF3 and kinase isogenic BaF3) were maintained in culture media at 37 ℃ with 5% CO_2 (100 ng/ml IL-3 was added to parental BaF3 cells). Cells were plated in 384-well culture plates (2000-6000/well for adherent cells; 10,000/well for suspension cells). Cell proliferation was determined after treatment with compounds for 72 h. Cell viability was measured by Cell Titer-Glo assay (Promega, USA) following manufacturer's instructions, and luminescence was measured in a multilabel reader (Envision2014, PerkinElmer, USA). IC_{50} values were determined by Prism 5.0.

Analysis of P-FLT3, P-STAT5, P-ERK and P-AKT *in Vitro*. To determine levels of P-FLT3, P-STAT5, P-ERK and P-AKT, cells were seeded in a 6-well cell culture plate at a density of 400000 cells per well for MV4-11 and incubated overnight in medium containing 10% fetal bovine serum (Life Technologies, Rockville, MD) in a total volume of 1800 μL. Then, 200 μL of serially diluted compounds were added to each well. Cell lysates were harvested after 4 h. FLT3/Phospho-FLT3$^{Tyr589/591}$, STAT5/Phospho-STAT5^{Tyr694}, AKT/Phospho-AKT^{Ser473}, ERK/Phosphop44/42MAPK(Erk1/2)$^{Thr202/Tyr204}$ and GAPDH antibody (Cell Signaling Technology) were used for immunoblotting.

PK Analysis. Male Sprague-Dawley rats (200-250 g) were used and randomly divided into two groups (n = 3 in each group). Rats were fasted 12 h before dosing and fasted 4 h after dosing. Compound **46** was administered by intravenous injection at a dose of 1 mg/kg or oral gavage at a dose of 5 mg/kg in saline mixture (DMSO/SolutolHS15/Saline = 5 : 10 : 85), respectively. Plasma

were collected into heparin tubes at time points post intravenous injection (5 min, 15 min, 30 min, 1 h, 2 h, 4 h, 8 h and 24 h). Plasma were collected into heparin tubes at time points post oral gavage (15 min, 30 min, 1 h, 2 h, 4 h, 8 h and 24 h). Compound concentrations were determined by Mass spectrometric analysis (API 4000/5500 LC-MS/MS). The relevant PK data was calculated with WinNonLin® 6.4 software.

***In Vivo* Efficacy for MV4−11 Xenografts.** Five to six-weeks-old female BALB/c mice (nu/nu) were purchased from Beijing Vital River Laboratory Animal Technology Co., Ltd (Beijing, China). All studies were carried out according to the animal-care regulations of Sundia Meditech Company, Ltd (Shanghai, China). Prior to implantation, cells were harvested during exponential growth. Approximately 4×10^7 MV4-11 cells in IDMEM medium were formulated as a 1:1 mixture with Matrigel (BD Biosciences, San Jose, CA), and injected into the subcutaneous space on the right flank of each nu/nu mouse in a total volume of 0.15 mL/mouse. Sorafenib was dissolved in a solution of anhydrous ethanol (50%) and polyoxyethylene 35 castor oil (50%). Compounds **40** and **46** were dissolved in a solution of PEG400 (2.5%), glucose (5%) and acetic acid/sodium acetate buffer (pH 4.5, 5%). Daily oral administration and intravenous injection were initiated when MV4-11 tumors had reached sizes of 153.60-224.26 mm^3. Animals were randomized into treatment groups of 8 mice each for efficacy studies. Sorafenib was treated orally with the dose of 40 mg/kg once daily for 14 days. Mice were dosed intravenously with vehicle, 20 and 40 mg/kg of compound **46** or 40 mg/kg of compound **40** twice daily for 14 days. Tumor growth was measured every 3 days using Vernier calipers for the duration of the treatment (Sundia Meditech Company, Ltd). The volume was calculated with the formula: tumor volume = $(a \times b^2)/2$, where a was the long diameter of tumor, and b was the short diameter of tumor. The percentage of tumor-growth inhibition (GI) was calculated with the formula: $GI = [1– (TV_t – TV_{initial})/(CV_t – CV_{initial})]\times 100\%$, where TV_t was the tumor volume measurement of the treatment group, $TV_{initial}$ was the tumor volume of the treatment group before administration, CVt was the tumor volume measurement of the solvent control group and $CV_{initial}$ was the tumor volume of the solvent control group before administration.

Metabolic Stability in Liver Microsomes. The metabolic stability of compound **40** and compound **46** (in human and rat liver microsomes) were tested by Nanjing MingJie Biotech Company. Solution of compound **46** (100 μM, 2.5 μL) or control working solution in DMSO and methanol (1 : 9) was added into microsome solution (0.5 mg/mL, 197.5 μL). After incubating the mixture at 37 °C for 5 min, NADPH solution (50 μL, 5 mM) was added. The final concentrations for test compound and microsome was 1 μM and 0.5 mg/mL, respectively. Every 30 μL of sample solution was taken out and terminated by a chilled mixture of Tolbutamide and Terfenadine (1 : 1) at 0 min, 5 min, 15 min, 30 min and 60 min, respectively. The mixture was vortexed for 1 min,

centrifuged at 4000 rpm for 15 min at 4 °C, and the supernatants were analyzed by LC-MS/MS (U3000-Qtrap6500). The data was analysis by the first order kinetics to calculate $t_{1/2}$ and Cl. The metabolic stability of compound **40** was tested in the same way to compound **46.**

Molecular Modeling. The FLT3 homology model was constructed as previously reported by us [23] and used here directly. The protein was prepared the Protein Preparation Wizard workflow in Schrödinger 2009 platform (Schrödinger, LLC, New York, NY). Compounds were docked into the FLT3 homology model using Glide module in a SP precision with default parameters. The docked poses were evaluated and ranked by default Glide score. The logP and Caco-2 cell permeability were predicted using Qikprop module in Schrödinger with the default settings.

HE Staining. The section was hydrated firstly, and then the section was dipped into a Coplin jar containing Mayer's hematoxylin and agitated for 3-5 min followed by rinsing with H_2O for 1 min. The section was dehydrated with 85% alcohol and 95% alcohol for 5 min each before it was stained with 1% eosin Y solution for 5 min with agitation. The alcohol was extracted with xylene for 5 min. Finally, one or two drops of mounting medium were added and covered with a coverslip.

KI-67 Staining. Tissue sections were quenched for endogenous peroxides, and then placed in an antigen retrieval solution (0.01 M citrate buffer, pH 6.0) for 15 min in a microwave oven at 600 W. Rabbit mAb anti-Ki-67 (CST (Shanghai) Biological Reagents Company Limited, China) was applied to the sections at dilutions of 1 : 50 and incubated overnight at 4 °C. The secondary detection system was added and incubated for 50 min. Staining was developed with DAB, and the slides were counterstained with hematoxylin for 3 min, dehydrated with xylene for 5 min, and mounted DPX Mounting Medium.

P-STAT5 Staining. Similar procedures with KI-67 staining were performed except that the phospho-Stat5 (Tyr694) (C11C5) rabbit mAb (CST (Shanghai) Biological Reagents Company Limited, China) was used as primary antibody.

TUNEL Staining. TUNEL staining was performed using in situ cell death detection kit, POD (#11684817910, Roche, Switzerland) according to the manufacturer's instructions. Firstly, sections were dewaxed in xylene, rehydrated in decreasing concentrations of ethanol (100%, 85%, 75%) and water, and then treated with Proteinase K (nuclease free) for 25 min at 37 °C. Mixture of terminal deoxynucleotidyl transferase and dUTP (1 : 9) in reaction buffer were applied to sections for 2 h at 37 °C. Following washes with PBS, the slides were covered by converter-POD solution for 30 min at 37 °C. Apoptotic cells were detected after incubation in DAPI chromogen (Servicebio technology, China) for approximately 10 min, and analyzed with camera equipped NIKON ECLIPSE C1 fluorescence microscope.

Acute toxicity of compound 46. The acute toxicity of compound **46** was determined in

SPFICR rats (4 animals for each group type of application, including 2 male and 2 female rats). The single dose of compound **46** was administrated intravenously (200 mg/kg, 150 mg/kg, 100 mg/kg) compared with solvent group, in which the injection volumes were all less than 0.5 mL. Mixture of acetic acid/sodium acetate buffer (pH 4.0, 5%), DMSO (2.5%) and H_2O (92.5%) was used as the solvent. And its toxicity was evaluated based on mortality. In addition, behavioral changes, clinical signs of intoxication and body weight changes were closely observed during the following 14 days. After intravenous administration of compound **46**, no signs of intoxication and no pathological macroscopic changes were recorded during the study. The maximum tolerated dose (MTD) of compound **46** after intravenous administration was determined to be higher than 200 mg/kg.

AUTHOR INFORMATION

Corresponding Authors

*(Shuai Lu) Tel: +86-25-86185153; Fax: +86-25-86185155; E-mail: lu_shuai@cpu.edu.cn

*(Yadong Chen) Tel: +86-25-86185169; Fax: +86-25-86185170; E-mail: chenyadong@gmail.com

Author Contributions

# Dr. Hao Heng, Dr. Hongmei Li and Dr. Zhijie Wang contributed equally. The authors declare no competing financial interest. The manuscript was written through contributions of all authors.

ACKNOWLEDGMENT

We are grateful to the Natural Science Foundation of Jiangsu Province (SBK2016020485), the National Natural Science Foundation of China (81502925), the “Double First-Class University project” (CPU2018GF02) of China Pharmaceutical University for financial support. Jiongheng Cai, Tianren Qin, Shuxian Wang and Li Xiang appreciate the College Students Innovation Project for the R&D of Novel Drugs (J1310032) from the National Found for Fostering Talents of Basic Science (NFFTBS). Dr. Jiewei Jiang read the manuscript critically and gave many valuable suggestions.

ABBREVIATIONS

FLT3, Fms-like receptor tyrosine kinase 3; AML, acute myeloid leukemia; RTK, receptor tyrosine kinase; SD, standard deviation; TKI, tyrosine kinase inhibitor; ITD, internal tandem duplication; IR, inhibition rate; r.t., Room temperature.

References

[1] A. Wang, X. Li, C. Chen, H. Wu, Z. Qi, C. Hu, K. Yu, J. Wu, J. Liu, X. Liu, Z. Hu, W. Wang, W. Wang, W. Wang, L. Wang, B. Wang, Q. Liu, L. Li, J. Ge, T. Ren, S. Zhang, R. Xia, J. Liu, Q. Liu, Discovery of 1-(4-(4-Amino-3-(4-(2-morpholinoethoxy)phenyl)-1H-pyrazolo[3,4-d]pyrimidin-1-yl)phenyl)-3-(5-(tert-butyl)isoxazol-3-yl)urea (CHMFL-FLT3-213) as a Highly Potent Type II FLT3 Kinase Inhibitor Capable of Overcoming a Variety of FLT3 Kinase Mutants in FLT3-ITD Positive AML,

Journal of medicinal chemistry, 60 (2017) 8407-8424.

[2] Leukemia− Acute Myeloid−AML:Statistics.http://www.cancer.net/cancer-types/leukemia-acute-myeloid-aml/statistics.

[3] C. Thiede, C. Steudel, B. Mohr, M. Schaich, U. Schakel, U. Platzbecker, M. Wermke, M. Bornhauser, M. Ritter, A. Neubauer, G. Ehninger, T. Illmer, Analysis of FLT3-activating mutations in 979 patients with acute myelogenous leukemia: association with FAB subtypes and identification of subgroups with poor prognosis, Blood, 99 (2002) 4326-4335.

[4] W.W. Li, X.Y. Wang, R.L. Zheng, H.X. Yan, Z.X. Cao, L. Zhong, Z.R. Wang, P. Ji, L.L. Yang, L.J. Wang, Y. Xu, J.J. Liu, J. Yang, C.H. Zhang, S. Ma, S. Feng, Q.Z. Sun, Y.Q. Wei, S.Y. Yang, Discovery of the novel potent and selective FLT3 inhibitor 1-{5-[7-(3-morpholinopropoxy)quinazolin-4-ylthio]-[1,3,4]thiadiazol-2-yl}-3-p-tolylurea and its anti-acute myeloid leukemia (AML) activities in vitro and in vivo, Journal of medicinal chemistry, 55 (2012) 3852-3866.

[5] S. Takahashi, Downstream molecular pathways of FLT3 in the pathogenesis of acute myeloid leukemia: biology and therapeutic implications, Journal of hematology & oncology, 4 (2011) 13.

[6] S. Kayser, R.F. Schlenk, M.C. Londono, F. Breitenbuecher, K. Wittke, J. Du, S. Groner, D. Spath, J. Krauter, A. Ganser, H. Dohner, T. Fischer, K. Dohner, A.M.L.S.G. German-Austrian, Insertion of FLT3 internal tandem duplication in the tyrosine kinase domain-1 is associated with resistance to chemotherapy and inferior outcome, Blood, 114 (2009) 2386-2392.

[7] H.K. Yukiya Yamamoto, Yasuyuki Nakano, Ritsuro Suzuki, Yoshihisa Kodera, Shuichi Miyawaki, Norio Asou, Kazutaka Kuriyama,Fumiharu Yagasaki, Chihiro Shimazaki, Hideki Akiyama, Kenji Saito, Miki Nishimura, Toshiko Motoji, Katsuji Shinagawa, Akihiro Takeshita, Hidehiko Saito, Ryuzo Ueda, Ryuzo Ohno, and Tomoki Naoe, Activating mutation of D835 within the activation loop of FLT3 in human hematologc malignancis, Blood, 97 (2001) 2434-2439.

[8] J. Cloos, B.F. Goemans, C.J. Hess, J.W. van Oostveen, Q. Waisfisz, S. Corthals, D. de Lange, N. Boeckx, K. Hahlen, D. Reinhardt, U. Creutzig, G.J. Schuurhuis, M. Zwaan Ch, G.J. Kaspers, Stability and prognostic influence of FLT3 mutations in paired initial and relapsed AML samples, Leukemia, 20 (2006) 1217-1220.

[9] S. Meshinchi, T.A. Alonzo, D.L. Stirewalt, M. Zwaan, M. Zimmerman, D. Reinhardt, G.J. Kaspers, N.A. Heerema, R. Gerbing, B.J. Lange, J.P. Radich, Clinical implications of FLT3 mutations in pediatric AML, Blood, 108 (2006) 3654-3661.

[10] R.E. Gale, C. Green, C. Allen, A.J. Mead, A.K. Burnett, R.K. Hills, D.C. Linch, P. Medical Research Council Adult Leukaemia Working, The impact of FLT3 internal tandem duplication mutant level, number, size, and interaction with NPM1 mutations in a large cohort of young adult patients with acute myeloid leukemia, Blood, 111 (2008) 2776-2784.

[11] R.F. Schlenk, K. Dohner, J. Krauter, S. Frohling, A. Corbacioglu, L. Bullinger, M. Habdank, D. Spath, M. Morgan, A. Benner, B. Schlegelberger, G. Heil, A. Ganser, H. Dohner, G. German-Austrian Acute Myeloid Leukemia Study, Mutations and treatment outcome in cytogenetically normal acute myeloid leukemia, The New England journal of medicine, 358 (2008) 1909-1918.

[12] Y.Y. Ke, V.K. Singh, M.S. Coumar, Y.C. Hsu, W.C. Wang, J.S. Song, C.H. Chen, W.H. Lin, S.H. Wu, J.T. Hsu, C. Shih, H.P. Hsieh, Homology modeling of DFG-in FMS-like tyrosine kinase 3 (FLT3) and structure-based virtual screening for inhibitor identification, Scientific reports, 5 (2015) 11702.

[13] R.M. Stone, S.J. Mandrekar, B.L. Sanford, K. Laumann, S. Geyer, C.D. Bloomfield, C. Thiede, T.W. Prior, K. Dohner, G. Marcucci, F. Lo-Coco, R.B. Klisovic, A. Wei, J. Sierra, M.A. Sanz, J.M.

Brandwein, T. de Witte, D. Niederwieser, F.R. Appelbaum, B.C. Medeiros, M.S. Tallman, J. Krauter, R.F. Schlenk, A. Ganser, H. Serve, G. Ehninger, S. Amadori, R.A. Larson, H. Dohner, Midostaurin plus Chemotherapy for Acute Myeloid Leukemia with a FLT3 Mutation, The New England journal of medicine, 377 (2017) 454-464.

[14] G. Borthakur, H.M. Kantarjian, S. O'Brien, G. Garcia-Manero, E. Jabbour, N. Daver, T.M. Kadia, R. Gborogen, M. Konopleva, M. Andreeff, F. Ravandi, J.E. Cortes, The Combination of Quizartinib with Azacitidine or Low Dose Cytarabine Is Highly Active in Patients (Pts) with FLT3-ITD Mutated Myeloid Leukemias: Interim Report of a Phase I/II Trial, Blood, 124 (2014) 388.

[15] L. Xuan, Y. Wang, F. Huang, E. Jiang, L. Deng, B. Wu, Z. Fan, X. Liang, N. Xu, J. Ye, R. Lin, C. Yin, Y. Zhang, J. Sun, M. Han, X. Huang, Q. Liu, Effect of sorafenib on the outcomes of patients with FLT3-ITD acute myeloid leukemia undergoing allogeneic hematopoietic stem cell transplantation, Cancer, 124 (2018) 1954-1963.

[16] A. Antar, M.A. Kharfan-Dabaja, R. Mahfouz, A. Bazarbachi, Sorafenib Maintenance Appears Safe and Improves Clinical Outcomes in FLT3-ITD Acute Myeloid Leukemia After Allogeneic Hematopoietic Cell Transplantation, Clinical lymphoma, myeloma & leukemia, 15 (2015) 298-302.

[17] T. De Freitas, S. Marktel, S. Piemontese, M.G. Carrabba, C. Tresoldi, C. Messina, M.T. Lupo Stanghellini, A. Assanelli, C. Corti, M. Bernardi, J. Peccatori, L. Vago, F. Ciceri, High rate of hematological responses to sorafenib in FLT3-ITD acute myeloid leukemia relapsed after allogeneic hematopoietic stem cell transplantation, European journal of haematology, 96 (2016) 629-636.

[18] Q.Y. Lan, Y.L. Zhi, H. Heng, J.Y. Tian, X.X. Guo, H.C. Liu, Y.D. Chen, T. Lu, S. Lu, Chemical Space of FLT3 Inhibitors as Potential Anti-AML Drugs, Recent Pat Anti-Canc, 12 (2017) 296-322.

[19] M.E. Percival, E. Estey, Emerging treatments in acute myeloid leukemia: current standards and unmet challenges, Clinical advances in hematology & oncology : H&O, 15 (2017) 632-642.

[20] C.C. Smith, E.A. Lasater, X. Zhu, K.C. Lin, W.K. Stewart, L.E. Damon, S. Salerno, N.P. Shah, Activity of ponatinib against clinically-relevant AC220-resistant kinase domain mutants of FLT3-ITD, Blood, 121 (2013) 3165-3171.

[21] Y. Wang, Y. Zhi, Q. Jin, S. Lu, G. Lin, H. Yuan, T. Yang, Z. Wang, C. Yao, J. Ling, H. Guo, T. Li, J. Jin, B. Li, L. Zhang, Y. Chen, T. Lu, Discovery of 4-((7H-Pyrrolo[2,3-d]pyrimidin-4-yl)amino)-N-(4-((4-methylpiperazin-1-yl)methyl)p henyl)-1H-pyrazole-3-carboxamide (FN-1501), an FLT3- and CDK-Kinase Inhibitor with Potentially High Efficiency against Acute Myelocytic Leukemia, Journal of medicinal chemistry, 61 (2018) 1499-1518.

[22] Y. Zhi, B. Li, C. Yao, H. Li, P. Chen, J. Bao, T. Qin, Y. Wang, T. Lu, S. Lu, Discovery of the selective and efficacious inhibitors of FLT3 mutations, Eur J Med Chem, 155 (2018) 303-315.

[23] H. Heng, Y. Zhi, H. Yuan, Z. Wang, H. Li, S. Wang, J. Tian, H. Liu, Y. Chen, T. Lu, T. Ran, S. Lu, Discovery of a highly selective FLT3 inhibitor with specific proliferation inhibition against AML cells harboring FLT3-ITD mutation, Eur J Med Chem, 163 (2018) 195-206.

[24] C.P. Miller, M. Shomali, C.R. Lyttle, L.S. O'Dea, H. Herendeen, K. Gallacher, D. Paquin, D.R. Compton, B. Sahoo, S.A. Kerrigan, M.S. Burge, M. Nickels, J.L. Green, J.A. Katzenellenbogen, A. Tchesnokov, G. Hattersley, Design, Synthesis, and Preclinical Characterization of the Selective Androgen Receptor Modulator (SARM) RAD140, ACS medicinal chemistry letters, 2 (2011) 124-129.

[25] N.M. Shaw, A.B. Naughton, The substrate specificity of the heat-stable stereospecific amidase from Klebsiella oxytoca, Tetrahedron, 60 (2004) 747-752.

[26] N. Lakshminarayana, Y.R. Prasad, L. Gharat, A. Thomas, S. Narayanan, A. Raghuram, C.V.

Srinivasan, B. Gopalan, Synthesis and evaluation of some novel dibenzo[b,d]furan carboxylic acids as potential anti-diabetic agents, Eur J Med Chem, 45 (2010) 3709-3718.

[27] A.A. Warkentin, M.S. Lopez, E.A. Lasater, K. Lin, B.L. He, A.Y. Leung, C.C. Smith, N.P. Shah, K.M. Shokat, Overcoming myelosuppression due to synthetic lethal toxicity for FLT3-targeted acute myeloid leukemia therapy, Elife, 3 (2014).

[28] A.T. Fathi, Y.B. Chen, The role of FLT3 inhibitors in the treatment of FLT3-mutated acute myeloid leukemia, Eur J Haematol, 98 (2017) 330-336.

[29] X. Liang, B. Wang, C. Chen, A. Wang, C. Hu, F. Zou, K. Yu, Q. Liu, F. Li, Z. Hu, T. Lu, J. Wang, L. Wang, E. Weisberg, L. Li, R. Xia, W. Wang, T. Ren, J. Ge, J. Liu, Q. Liu, Discovery of N-(4-(6-acetamidopyrimidin-4-yloxy)phenyl)-2-(2-(trifluoromethyl)phenyl)acetamide (CHMFL-FLT3-335) as a Potent Fms-like Tyrosine Kinase 3 Internal Tandem Duplications (FLT3-ITD) Mutant Selective Inhibitor for Acute Myeloid Leukemia, Journal of medicinal chemistry, (2018).

[30] Y. Chen, Y. Pan, Y. Guo, W. Zhao, W.T. Ho, J. Wang, M. Xu, F.C. Yang, Z.J. Zhao, Tyrosine kinase inhibitors targeting FLT3 in the treatment of acute myeloid leukemia, Stem Cell Investig, 4 (2017) 48.

[31] W. Zhang, C. Gao, M. Konopleva, Y. Chen, R.O. Jacamo, G. Borthakur, J.E. Cortes, F. Ravandi, A. Ramachandran, M. Andreeff, Reversal of acquired drug resistance in FLT3-mutated acute myeloid leukemia cells via distinct drug combination strategies, Clin Cancer Res, 20 (2014) 2363-2374.

[32] E. Weisberg, R. Barrett, Q. Liu, R. Stone, N. Gray, J.D. Griffin, FLT3 inhibition and mechanisms of drug resistance in mutant FLT3-positive AML, Drug resistance updates : reviews and commentaries in antimicrobial and anticancer chemotherapy, 12 (2009) 81-89.

[33] D. Auclair, D. Miller, V. Yatsula, W. Pickett, C. Carter, Y. Chang, X. Zhang, D. Wilkie, A. Burd, H. Shi, S. Rocks, R. Gedrich, L. Abriola, H. Vasavada, M. Lynch, J. Dumas, P.A. Trail, S.M. Wilhelm, Antitumor activity of sorafenib in FLT3-driven leukemic cells, Leukemia, 21 (2007) 439-445.

ACCEPTED MANUSCRIPT

Highlights:

- **46** was highly potent and specific against FLT3-ITD.
- **46** showed good antitumor efficacy in MV4-11 mouse xenograft model without decreasing the body weight of mice.

ACCEPTED MANUSCRIPT